Inorg. Chem. **2007**, *46*, 4718–4732

Synthesis, Structure, and Luminescence of Di- and Trinuclear Palladium/Gold and Platinum/Gold Complexes with (2,7-Di-*tert*-butylfluoren-9-ylidene)methanedithiolate[†,1]

José Vicente, Pablo González-Herrero,* and María Pérez-Cadenas

Grupo de Química Organometálica, Departamento de Química Inorgánica, Facultad de Química, Universidad de Murcia, Apdo. 4021, 30071 Murcia, Spain

Peter G. Jones

Institut für Anorganische und Analytische Chemie, Technische Universität Braunschweig, Postfach 3329, 38023 Braunschweig, Germany

Delia Bautista

SACE, Universidad de Murcia, Apdo. 4021, 30071 Murcia, Spain

Received January 30, 2007

Acetone solutions of $[Au(OClO_3)(PCy_3)]$ react with complexes $[M\{S_2C{=}(t\text{-Bu-fy})\}_2]^{2-}$ [*t*-Bu-fy = 2,7-di-*tert*-butylfluoren-9-ylidene; M = Pd (**2a**), Pt (**2b**)] or $[M\{S_2C{=}(t\text{-Bu-fy})\}(dbbpy)]$ [dbbpy = 4,4′-di-*tert*-butyl-2,2′-bipyridyl; M = Pd (**3a**), Pt (**3b**)] to give the heteronuclear complexes $[M\{S_2C{=}(t\text{-Bu-fy})\}_2\{Au(PCy_3)\}_2]$ [2:1 molar ratio; M = Pd (**4a**), Pt (**4b**)], $[M\{S_2C{=}(t\text{-Bu-fy})\}(dbbpy)\{Au(PCy_3)\}]ClO_4$ [1:1 molar ratio; M = Pd (**5a**), Pt (**5b**)], or $[M\{S_2C{=}(t\text{-Bu-fy})\}(dbbpy)\{Au(PCy_3)\}_2](ClO_4)_2$ [2:1 molar ratio; M = Pd (**6a**), Pt (**6b**)]. The crystal structures of **3a**, **4a**, **4b**, **5b**, and **6a** have been solved by single-crystal X-ray studies and, in the cases of the heteronuclear derivatives, reveal the formation of short Pd···Au or Pt···Au metallophilic contacts in the range of 3.048–3.311 Å. Compounds **4a** and **b** and **5a** and **b** undergo a dynamic process in solution that involves the migration of the $[Au(PCy_3)]^+$ units between the sulfur atoms of the dithiolato ligands. The coordination of **2a** and **b** and **3a** and **b** to $[Au(PCy_3)]^+$ units results in important modifications of their photophysical properties. The dominant effect in the absorption spectra is an increase in the energy of the MLCT (**4a** and **b**) or charge transfer to diimine (**5a**, **b**, **6a**, **b**) transitions because of a decrease in the energies of the mixed metal/dithiolate HOMOs. The Pd complexes **2a** and **4a** are luminescent at 77 K, and the features of their emissions are consistent with an essentially metal-centered ^{3}d–d state. The Pt/Au complexes are also luminescent at 77 K, and their emissions can be assigned as originating from a MLCT triplet state (**4b**) or a mixture of charge transfer to diimine and diimine intraligand π–π^* triplet states (**5b** and **6b**).

Introduction

The interest in heterometallic complexes, aggregates, and clusters has grown steadily during the last two decades.[2−5] Many of the recent studies in this area have been stimulated by the intriguing photophysical properties of these materials, which in many cases have their origin in metallophilic interactions between metal ions with closed or pseudoclosed shell electronic configurations (d^{10}, d^8, s^2).[6,7] Such interactions have thus been acknowledged not only as essential factors in the molecular and surpramolecular structures, but also as having implications for certain biochemical systems and technological applications.[8]

* To whom correspondence should be addressed. E-mail: jvs1@um.es (J.V.); pgh@um.es (P.G.-H.). http://www.um.es/gqo/.

† Dedicated to Professor Miguel Yus on the occasion of his 60th birthday.

(1) (Fluoren-9-ylidene)methanedithiolato Complexes, Part 4. For previous parts, see refs 16−18.

(2) (a) Balch, A. L.; Catalano, V. J.; Noll, B. C.; Olmstead, M. M. *J. Am. Chem. Soc.* **1990**, *112*, 7558−7566. (b) Assefa, Z.; Destefano, F.; Garepapaghi, M. A.; Lacasce, J. H.; Ouellete, S.; Corson, M. R.; Nagle, J. K.; Patterson, H. H. *Inorg. Chem.* **1991**, *30*, 2868−2876. (c) Balch, A. L.; Neve, F.; Olmstead, M. M. *J. Am. Chem. Soc.* **1991**, *113*, 2995−3001. (d) Balch, A. L.; Catalano, V. J. *Inorg. Chem.* **1991**, *30*, 1302−1308. (e) Yip, H. K.; Lin, H. M.; Wang, Y.; Che, C. M. *Inorg. Chem.* **1993**, *32*, 3402−3407. (f) Yip, H. K.; Lin, H. M.; Cheung, K. K.; Che, C. M.; Wang, Y. *Inorg. Chem.* **1994**, *33*, 1644−1651. (g) Yam, V. W. W.; Lo, W. Y.; Zhu, N. Y. *Chem. Commun.* **2003**, 2446−2447. (h) Chen, Y. D.; Zhang, U. Y.; Qin, Y. H.; Chen, Z. N. *Inorg. Chem.* **2005**, *44*, 6456−6462. (i) Stork, J. R.; Olmstead, M. M.; Balch, A. L. *J. Am. Chem. Soc.* **2005**, *127*, 6512−6513. (j) Stork, J. R.; Olmstead, M. M.; Fettinger, J. C.; Balch, A. L. *Inorg. Chem.* **2006**, *45*, 849−857. (k) Shin, R. Y. C.; Tan, G. K.; Koh, L. L.; Vittal, J. J.; Goh, L. Y.; Webster, R. D. *Organometallics* **2005**, *24*, 539−551.

10.1021/ic070164h CCC: $37.00
Published on Web 04/13/2007

1,1-Ethylenedithiolates ($XYC{=}CS_2^{2-}$) have long been recognized for their ability to form clusters[9] and heteropolynuclear complexes,[10] and some of them are also capable of making use of multiple donor atoms to form coordination polymers.[11,12] We have recently shown that Pd(II) and Pt(II) complexes of the type $[M\{S_2C{=}(COMe)_2\}L_2]$, with M = Pd, Pt and L = PPh_3, *t*-BuNC or L_2 = 1,5-cyclooctadiene, can act as metalloligands toward Ag(I) and Au(I) centers to form a variety of heterodinuclear, trinuclear, and tetranuclear structures that display $d^8{-}d^{10}$ short contacts.[13−15] Our research group has also undertaken the study of the reactivity and photophysical properties of transition metal complexes with (fluoren-9-ylidene)methanedithiolate and several disubstituted derivatives.[16−18] These new ligands exhibit significant differences with respect to the majority of 1,1-ethylenedithiolates described to date, which are attributable to the presence of the extensively conjugated fluoren-9-ylidene fragment and the absence of electron-withdrawing functional groups, and affect the reactivity and photophysical properties of their metal complexes. Thus, the strongly electron-donating character of these ligands is responsible for the facile oxidation of certain Au(I) and Pt(II) complexes under atmospheric conditions, and the unusually low energies of their charge-transfer absorptions and emissions.[16,18] We have also reported the aerial oxidation of Cu(I) and Cu(II) complexes with (2,7-di-*tert*-butylfluoren-9-ylidene)methanedithiolate [(*t*-Bu-fy)$=CS_2^{2-}$] and the oxidatively promoted condensation of the ligand in the coordination sphere of Cu(I).[17]

In this paper, we describe the structures, dynamic behavior in solution, and photophysical properties of a series of Pd/Au and Pt/Au heterodinuclear and trinuclear complexes with the (*t*-Bu-fy)$=CS_2^{2-}$ ligand, obtained through the aggregation of $[Au(PCy)_3]^+$ units to $[M\{S_2C{=}(t\text{-Bu-fy})\}_2]^{2-}$ or $[M\{S_2C{=}(t\text{-Bu-fy})\}(dbbpy)]$ (M = Pd, Pt; dbbpy = 4,4′-di-*tert*-butyl-2,2′-bipyridyl). These precursors belong to the basic types $[M(1,1\text{-dithiolate})_2]^{2-}$ and [M(1,1-dithiolate)(diimine)], which, for M = Pt, have been the subject of previous intensive research because of their interesting excited-state properties.[19−23] The present work is mainly aimed at the evaluation of metal aggregation as a method of obtaining compounds with enhanced or modified luminescent properties.

Experimental Section

General Considerations. Materials and Instrumentation. All preparations were carried out at room temperature unless otherwise stated. Solvents were dried by standard methods. The ligand precursor piperidinium 2,7-di-*tert*-butyl-9*H*-fluorene-9-carbodithio-

(3) (a) Yip, H. K.; Che, C. M.; Peng, S. M. *J. Chem. Soc., Chem. Commun.* **1991**, 1626−1628. (b) Yip, H. K.; Lin, H. M.; Wang, Y.; Che, C. M. *J. Chem. Soc., Dalton Trans.* **1993**, 2939−2944.

(4) (a) Chen, Y. D.; Qin, Y. H.; Zhang, L. Y.; Shi, L. X.; Chen, Z. N. *Inorg. Chem.* **2004**, *43*, 1197−1205. (b) Chen, Y. D.; Zhang, L. Y.; Shi, L. X.; Chen, Z. N. *Inorg. Chem.* **2004**, *43*, 7493−7501.

(5) Stork, J. R.; Rios, D.; Pham, D.; Bicocca, V.; Olmstead, M. M.; Balch, A. L. *Inorg. Chem.* **2005**, *44*, 3466−3472.

(6) Pyykkö, P. *Chem. Rev.* **1997**, *97*, 597−636.

(7) (a) Che, C. M.; Lai, S. W. *Coord. Chem. Rev.* **2005**, *249*, 1296−1309. (b) de la Riva, H.; Nieuwhuyzen, M.; Fierro, C. M.; Raithby, P. R.; Male, L.; Lagunas, M. C. *Inorg. Chem.* **2006**, *45*, 1418−1420. (c) Fernández, E. J.; Jones, P. G.; Laguna, A.; López-de-Luzuriaga, J. M.; Monge, M.; Pérez, J.; Olmos, M. E. *Inorg. Chem.* **2002**, *41*, 1056−1063. (d) Fernández, E. J.; López-de-Luzuriaga, J. M.; Monge, M.; Olmos, M. E.; Pérez, J.; Laguna, A. *J. Am. Chem. Soc.* **2002**, *124*, 5942−5943. (e) Kishimura, A.; Yamashita, T.; Aida, T. *J. Am. Chem. Soc.* **2005**, *127*, 179−183. (f) Rawashdeh-Omary, M. A.; Omary, M. A.; Fackler, J. P. *Inorg. Chim. Acta* **2002**, *334*, 376−384. (g) Rawashdeh-Omary, M. A.; Omary, M. A.; Fackler, J. P., Jr.; Galassi, R.; Pietroni, B. R.; Burini, A. *J. Am. Chem. Soc.* **2001**, *123*, 9689−9691. (h) Yam, V. W. W.; Yu, K. L.; Wong, K. M. C.; Cheung, K. K. *Organometallics* **2001**, *20*, 721−726. (i) Gade, L. H. *Angew. Chem., Int. Ed.* **2001**, *40*, 3573. (j) Yam, V. W. W.; Yu, K. L.; Cheng, E. C. C.; Yeung, P. K. Y.; Cheung, K. K.; Zhu, N. Y. *Chem.−Eur. J.* **2002**, *8*, 4121−4128. (k) Fernández, E. J.; López-de-Luzuriaga, J. M.; Olmos, M. E.; Pérez, J.; Laguna, A.; Lagunas, M. C. *Inorg. Chem.* **2005**, *44*, 6012−6018. (l) Berenguer, J. R.; Forniés, J.; Gil, B.; Lalinde, E. *Chem.−Eur. J.* **2006**, *12*, 785−795. (m) Gil, B.; Forniés, J.; Gómez, J.; Lalinde, E.; Martín, A.; Moreno, M. T. *Inorg. Chem.* **2006**, *45*, 7788−7798.

(8) (a) Yam, V. W. W.; Lo, K. K. W. *Chem. Soc. Rev.* **1999**, *28*, 323−334. (b) Ma, Y. G.; Che, C. M.; Chao, H. Y.; Zhou, X. M.; Chan, W. H.; Shen, J. C. *Adv. Mater.* **1999**, *11*, 852−857. (c) Hayoun, R.; Zhong, D. K.; Rheingold, A. L.; Doerrer, L. H. *Inorg. Chem.* **2006**, *45*, 6120−6122. (d) Fernández, E. J.; Laguna, A.; López-de-Luzuriaga, J. M.; Monge, M.; Montiel, M.; Olmos, M. E.; Rodríguez-Castillo, M. *Organometallics* **2006**, *25*, 3639−3646.

(9) (a) Liu, C. W.; Liaw, B. J.; Wang, J. C.; Liou, L. S.; Keng, T. C. *J. Chem. Soc., Dalton Trans.* **2002**, 1058−1065. (b) Su, W. P.; Hong, M. C.; Weng, J. B.; Liang, Y. C.; Zhao, Y. J.; Cao, R.; Zhou, Z. Y.; Chan, A. S. C. *Inorg. Chim. Acta* **2002**, *331*, 8−15. (c) Liu, C. W.; Liaw, B. J.; Wang, J. C.; Keng, T. C. *Inorg. Chem.* **2000**, *39*, 1329−1332. (d) Liu, C. W.; Staples, R. J.; Fackler, J. P. *Coord. Chem. Rev.* **1998**, *174*, 147−177. (e) Su, W. P.; Hong, M. C.; Cao, R.; Chen, J. T.; Wu, D. X.; Liu, H. Q.; Lu, J. X. *Inorg. Chim. Acta* **1998**, *267*, 313−317. (f) Hong, M. C.; Su, W. P.; Cao, R.; Jiang, F. L.; Liu, H. Q.; Lu, J. X. *Inorg. Chim. Acta* **1998**, *274*, 229−231. (g) Fackler, J. P.; Staples, R. J.; Liu, C. W.; Stubbs, R. T.; Lopez, C.; Pitts, J. T. *Pure Appl. Chem.* **1998**, *70*, 839−844. (h) Coucouvanis, D.; Swenson, D.; Baenziger, N. C.; Pedelty, R.; Caffery, M. L.; Kanodia, S. *Inorg. Chem.* **1989**, *28*, 2829−2836. (i) Dietrich, H.; Storck, W.; Manecke, G. *J. Chem. Soc., Chem. Commun.* **1982**, 1036−1037. (j) Birker, P. J. M. W. L.; Verschoor, G. C. *J. Chem. Soc., Chem. Commun.* **1981**, 322−324. (k) McCandlish, L. E.; Bissell, E. C.; Coucouvanis, D.; Fackler, J. P.; Knox, K. *J. Am. Chem. Soc.* **1968**, *90*, 7357−7359. (l) Hollander, F. J.; Coucouvanis, D. *J. Am. Chem. Soc.* **1977**, *99*, 6268−6280.

(10) (a) Caffery, M. L.; Coucouvanis, D. *J. Inorg. Nucl. Chem.* **1975**, *37*, 2081−2086. (b) Coucouvanis, D.; Baenziger, N. C.; Johnson, S. M. *Inorg. Chem.* **1974**, *13*, 1191−1199.

(11) Zhu, Y. B.; Lu, S. F.; Huang, X. Y.; Wu, Q. J.; Yu, R. M.; Huang, J. Q. *Acta Crystallogr., Sect. C: Cryst. Struct. Commun.* **1995**, *51*, 1515−1517.

(12) Long, D. L.; Chen, J. T.; Cui, Y.; Huang, J. S. *Chem. Lett.* **1998**, 171−172.

(13) Vicente, J.; Chicote, M. T.; Huertas, S.; Bautista, D.; Jones, P. G.; Fischer, A. K. *Inorg. Chem.* **2001**, *40*, 2051−2057.

(14) Vicente, J.; Chicote, M. T.; Huertas, S.; Jones, P. G.; Fischer, A. K. *Inorg. Chem.* **2001**, *40*, 6193−6200.

(15) Vicente, J.; Chicote, M. T.; Huertas, S.; Jones, P. G. *Inorg. Chem.* **2003**, *42*, 4268−4274.

(16) Vicente, J.; González-Herrero, P.; García-Sánchez, Y.; Jones, P. G.; Bardají, M. *Inorg. Chem.* **2004**, *43*, 7516−7531.

(17) Vicente, J.; González-Herrero, P.; García-Sánchez, Y.; Jones, P. G.; Bautista, D. *Eur. J. Inorg. Chem.* **2006**, 115−126.

(18) Vicente, J.; González-Herrero, P.; Pérez-Cadenas, M.; Jones, P. G.; Bautista, D. *Inorg. Chem.* **2005**, *44*, 7200−7213.

(19) Cummings, S. D.; Eisenberg, R. *Inorg. Chim. Acta* **1996**, *242*, 225−231.

(20) (a) Zuleta, J. A.; Chesta, C. A.; Eisenberg, R. *J. Am. Chem. Soc.* **1989**, *111*, 8916−8917. (b) Zuleta, J. A.; Burberry, M. S.; Eisenberg, R. *Coord. Chem. Rev.* **1990**, *97*, 47−64. (c) Bevilacqua, J. M.; Eisenberg, R. *Inorg. Chem.* **1994**, *33*, 2913−2923. (d) Paw, W.; Cummings, S. D.; Mansour, M. A.; Connick, W. B.; Geiger, D. K.; Eisenberg, R. *Coord. Chem. Rev.* **1998**, *171*, 125−150. (e) Hissler, M.; McGarrah, J. E.; Connick, W. B.; Geiger, D. K.; Cummings, S. D.; Eisenberg, R. *Coord. Chem. Rev.* **2000**, *208*, 115−137.

(21) Zuleta, J. A.; Bevilacqua, J. M.; Rehm, J. M.; Eisenberg, R. *Inorg. Chem.* **1992**, *31*, 1332−1337.

(22) Huertas, S.; Hissler, M.; McGarrah, J. E.; Lachicotte, R. J.; Eisenberg, R. *Inorg. Chem.* **2001**, *40*, 1183−1188.

(23) Cummings, S. D.; Eisenberg, R. *J. Am. Chem. Soc.* **1996**, *118*, 1949−1960.

Table 1. Crystallographic Data for **3a**·CH_2Cl_2, **4a**, **4b**, **5b**·Me_2CO, and **6a**·THF·C_6H_{14}

	3a·CH_2Cl_2	**4a**	**4b**	**5b**·Me_2CO	**6a**·THF·C_6H_{14}
formula	$C_{41}H_{50}Cl_2N_2PdS_2$	$C_{80}H_{114}Au_2P_2PdS_4$	$C_{80}H_{114}Au_2P_2PtS_4$	$C_{61}H_{87}AuClN_2O_5PPtS_2$	$C_{83}H_{129}Au_2Cl_2N_2O_9P_2PdS_2$
fw	812.25	1766.22	1854.91	1450.92	1996.18
T (K)	133(2)	100.2(2)	100.2(2)	100.2(2)	100.2(2)
λ (Å)	0.71073	0.71073	0.71073	0.71073	0.71073
cryst syst	monoclinic	monoclinic	monoclinic	orthorhombic	monoclinic
space group	$P2_1/c$	$P2_1/c$	$P2_1/c$	$Pbca$	$P2_1/n$
a (Å)	11.3930(11)	9.5339(4)	9.5454(4)	20.3656(9)	22.6833(9)
b (Å)	17.702(2)	15.1567(7)	15.1537(7)	17.0378(7)	14.4450(6)
c (Å)	19.709(2)	26.6961(12)	26.6997(11)	35.8373(16)	28.7838(12)
β (deg)	97.997(5)	92.012(2)	91.988(2)	90	112.831(2)
V (Å^3)	3936.1(7)	3855.3(3)	3859.7(3)	12435.0(9)	8692.4(6)
Z	4	2	2	8	4
ρ_{calcd} (Mg m^{-3})	1.371	1.521	1.596	1.550	1.525
μ (mm^{-1})	0.744	4.218	5.790	4.787	3.772
R1[a]	0.0389	0.0227	0.0429	0.0207	0.0313
wR2[b]	0.1138	0.0518	0.0776	0.0477	0.0731

[a] $R1 = \sum||F_o| - |F_c||/\sum|F_o|$ for reflections with $I > 2\sigma(I)$. [b] $wR2 = [\sum[w(F_o^2 - F_c^2)^2]/\sum[w(F_o^2)^2]]^{0.5}$ for all reflections; $w^{-1} = \sigma^2(F^2) + (aP)^2 + bP$, where $P = (2F_c^2 + F_o^2)/3$ and a and b are constants set by the program.

ate (**1**) was prepared as reported.[24] [$PdCl_2$(dbbpy)] was prepared by refluxing a suspension of *cis*-[$PtCl_2(DMSO)_2$][25] and 1 equiv of dbbpy in acetone. The complexes $(Pr_4N)_2$[Pt{S_2C═(*t*-Bu-fy)}$_2$] (**2b**),[18] [Pt{S_2C═(*t*-Bu-fy)}(dbbpy)] (**3b**),[18] and [AuCl(PCy_3)][16] were prepared following the published procedures. All other reagents were obtained from commercial sources and used without further purification. NMR spectra were recorded on Bruker Avance 200, 300, 400, or 600 spectrometers, usually at 298 K unless otherwise indicated. Chemical shifts are referred to internal TMS (^{1}H and ^{13}C{H}) or external 85% H_3PO_4 (^{31}P{H}). The ^{13}C{H} NMR resonances of the Pr_4N^+ cation are not given. The assignments of the ^{1}H and ^{13}C{H} NMR spectra were made with the help of HMBC and HSQC experiments. Melting points were determined on a Reichert apparatus and are uncorrected. Elemental analyses were carried out with a Carlo Erba 1106 microanalyzer. Infrared spectra were recorded in the range of 4000−200 cm^{-1} on a Perkin-Elmer 16F PC FT-IR spectrophotometer using Nujol mulls between polyethylene sheets. UV−vis absorption spectra were recorded on an Unicam UV500 spectrophotometer. Excitation and emission spectra were recorded on a Jobin Yvon Fluorolog 3−22 spectrofluorometer with a 450 W xenon lamp, double-grating monochromators, and a TBX-04 photomultiplier. The solid-state measurements were made in a front-face configuration using polycrystalline samples between quartz coverslips; the solution measurements were carried out in a right angle configuration using degassed solutions of the samples in 10 mm quartz fluorescence cells or 5 mm quartz NMR tubes. The solvents used were CH_2Cl_2 at 298 K and CH_2Cl_2, DMM (DMF/CH_2Cl_2/MeOH 1:1:1), or toluene at 77 K, as specified. For the low-temperature measurements, a liquid nitrogen Dewar with quartz windows or an Oxford Instruments Optistat-DN cryostat were employed. Lifetimes were measured using the Fluorolog's FL-1040 phosphorimeter accessory.

X-ray Structure Determinations. Crystals of **3a**·CH_2Cl_2, **4a**, **4b**, **5b**·Me_2CO, and **6a**·THF·C_6H_{14} suitable for X-ray diffraction studies were obtained by the liquid−liquid diffusion method from CH_2Cl_2/Et_2O, Me_2CO/Et_2O or THF/*n*-hexane. Numerical details are presented in Table 1. Data for **4a**, **b**, **5b**·Me_2CO, and **6a**·THF·C_6H_{14} were recorded on a Bruker Smart APEX diffractometer. The structures of **4a** and **6a**·THF·C_6H_{14} were solved by direct methods, and those of **4b** and **5b**·Me_2CO were solved by the heavy atom method. All of them were refined anisotropically on F^2 using the program SHELXL-97 (G. M. Sheldrick, University of Göttingen). Restraints to local aromatic ring symmetry or light atom displacement factor components were applied in some cases. Hydrogen atoms were included using rigid methyl groups or a riding model.

Special Features of Refinement. For compound **3a**, the dichloromethane molecule is disordered over two positions with a relative occupancy of ∼4:1. For compound **5b**, the Me groups of one of the *t*-Bu groups are disordered over two positions (∼73:27).

Caution! Perchlorate salts of metal complexes with organic ligands are potentially explosive. Preparations on a larger scale than that described here should be avoided.

$(Pr_4N)_2$[Pd{S_2C═(*t*-Bu-fy)}$_2$] (2a). Piperidine (100 μL, 1.01 mmol) and Pr_4NCl (160 mg, 0.72 mmol) were added to a stirred suspension of $PdCl_2$ (52 mg, 0.29 mmol) in CH_2Cl_2 (15 mL). A turbid, pale yellow solution formed, which was filtered through Celite to remove small amounts of insoluble material. The addition of dithioate **1** (301 mg, 0.63 mmol) led to immediate reaction with precipitation of an orange solid, which was filtered off, washed with CH_2Cl_2 (4 mL), and vacuum-dried to give **2a**. Yield: 164 mg, 47%. Anal. Calcd for $C_{68}H_{104}N_2PdS_4$: C, 68.97; H, 8.85; N, 2.37; S, 10.83. Found: C, 68.74; H, 8.91; N, 2.53; S, 10.58. mp: 230−240 °C (dec). IR (Nujol, cm^{-1}): ν(C═CS_2), 1500; ν(Pd−S), 342. ^{1}H NMR [400.9 MHz, $(CD_3)_2SO$]: δ 8.97 (d, $^4J_{HH}$ = 1.6 Hz, 4 H, H1, H8), 7.62 (d, $^3J_{HH}$ = 8.0 Hz, 4 H, H4, H5), 7.08 (dd, $^3J_{HH}$ = 8.0 Hz, $^4J_{HH}$ = 1.6 Hz, 4 H, H3, H6), 3.10 (m, NCH_2, 16 H), 1.58 (m, CH_2, 16 H), 1.35 (s, 36 H, *t*-Bu), 0.87 (t, $^3J_{HH}$ = 7.2 Hz, 24 H, Me, Pr_4N^+). ^{13}C{^{1}H} NMR [100.8 MHz, $(CD_3)_2SO$]: δ 185.6 (CS_2), 146.9 (C2, C7), 139.2 (C8a, C9a), 131.7 (C4a, C4b), 124.0 (C9), 119.5 (C4, C5), 118.6 (C3, C6), 117.4 (C1, C8), 34.6 (*C*Me_3), 31.8 (C*Me*$_3$).

[Pd{S_2C═(*t*-Bu-fy)}(dbbpy)] (3a). Piperidine (17 μL, 0.17 mmol) and dithioate **1** (76 mg, 0.16 mmol) were added to a suspension of [$PdCl_2$(dbbpy)] (65 mg, 0.15 mmol) in CH_2Cl_2 (15 mL). The resulting red solution was stirred for 10 min and concentrated to ∼2 mL. The addition of Et_2O (40 mL) led to the precipitation of a dark red solid, which was filtered off, washed with methanol (2 × 2 mL) and Et_2O (4 mL), and vacuum-dried to give **3a**. Yield: 85 mg, 80%. Anal. Calcd for $C_{40}H_{48}N_2PdS_2$: C, 66.05; H, 6.65; N, 3.85; S, 8.82. Found: C, 65.74; H, 6.72; N, 4.02; S, 8.68. mp: 220 °C. IR (Nujol, cm^{-1}): ν(C═CS_2), 1536. ^{1}H NMR (400.9 MHz, $CDCl_3$): δ 8.83 (d, $^4J_{HH}$ = 1.4 Hz, 2 H, H1, H8), 8.54 (d, $^3J_{HH}$ = 5.7 Hz, 2 H, H6, dbbpy), 8.06 (d, $^4J_{HH}$ = 1.5 Hz, 2 H, H3, dbbpy), 7.67 (d, $^3J_{HH}$ = 7.9 Hz, 2 H, H4, H5),

(24) Vicente, J.; González-Herrero, P.; García-Sánchez, Y.; Pérez-Cadenas, M. *Tetrahedron Lett.* **2004**, *45*, 8859−8861.
(25) Kukushkin, V. Y.; Pombeiro, A. J. L.; Ferreira, C. M. P.; Elding, L. I. *Inorg. Synth.* **2002**, *33*, 189−196.

7.53 (dd, $^4J_{HH}$ = 1.8 Hz, $^3J_{HH}$ = 5.7 Hz, 2 H, H5, dbbpy), 7.26 (dd, $^4J_{HH}$ = 1.7 Hz, $^3J_{HH}$ = 7.9 Hz, 2 H, H3, H6), 1.46 (s, 18 H, *t*-Bu, dithiolato), 1.43 (s, 18 H, *t*-Bu, dbbpy). $^{13}C\{^1H\}$ NMR (100.8 MHz, $CDCl_3$): δ 163.8 (C4, dbbpy), 162.4 (CS_2), 154.6 (C2, dbbpy), 148.5 (C2, C7, dithiolato + C6, dbbpy), 139.4 (C8a, C9a), 134.6 (C4a, C4b), 127.9 (C9), 123.9 (C5, dbbpy), 121.2 (C3, C6), 119.5 (C1, C8), 119.1 (C3, dbbpy), 117.9 (C4, C5), 35.7 (*C*Me$_3$, dbbpy), 34.9 (*C*Me$_3$, dithiolato), 31.9 (C*Me$_3$*, dithiolato), 30.3 (C*Me$_3$*, dbbpy).

[Pd{S$_2$C=(*t*-Bu-fy)}$_2${Au(PCy$_3$)}$_2$] (4a). $AgClO_4$ (53 mg, 0.23 mmol) was added to a stirred suspension of [AuCl(PCy$_3$)] (118 mg, 0.23 mmol) in acetone (10 mL). After 10 min, the mixture was filtered through Celite to remove the precipitate of AgCl. Compound **2a** (133 mg, 0.11 mmol) was then added to the clear filtrate, and the mixture was stirred for 30 min. A yellow solid precipitated, which was filtered off, washed with acetone (5 mL), recrystallized from CH_2Cl_2/Et_2O, and vacuum-dried to give **4a**. Yield: 136 mg, 88%. Anal. Calcd for $C_{80}H_{114}Au_2P_2PdS_4$: C, 54.40; H, 6.51; S, 7.26. Found: C, 54.38; H, 6.87; S, 7.12. mp: 200 °C (dec). IR (Nujol, cm^{-1}): ν(C=CS$_2$), 1538; ν(Pd−S), 354, 334. ^{1}H NMR (400.9 MHz, $CDCl_3$): δ 8.91 (d, $^4J_{HH}$ = 1.8 Hz, 4 H, H1, H8), 7.61 (d, $^3J_{HH}$ = 8.0 Hz, 4 H, H4, H5), 7.93 (dd, $^3J_{HH}$ = 8.0 Hz, $^4J_{HH}$ = 1.8 Hz, 4 H, H3, H6), 2.04−1.91 (br m, 18 H, Cy), 1.67 (br m, 12 H, Cy), 1.57−1.48 (br m, 18 H Cy), 1.40 (s, 18 H, *t*-Bu), 1.19−1.12 (br m, 18 H, Cy). $^{13}C\{^1H\}$ NMR (100.8 MHz, $CDCl_3$): δ 158.7 (CS_2), 148.6 (C2, C7), 139.1 (C8a, C9a), 135.2 (C4a, C4b), 131.6 (C9), 121.8 (C3, C6), 121.7 (C1, C8), 117.7 (C4, C5), 35.0 (*C*Me$_3$), 33.4 (d, $^1J_{CP}$ = 27.6 Hz, C1, Cy), 31.8 (C*Me$_3$*), 30.7 (C2, C6, Cy), 27.0 (d, $^3J_{CP}$ = 12.1 Hz, C3, C5, Cy), 25.7 (C4, Cy). $^{31}P\{^1H\}$ NMR (162.3 MHz, $CDCl_3$): δ 57.4.

[Pt{S$_2$C=(*t*-Bu-fy)}$_2${Au(PCy$_3$)}$_2$] (4b). This yellow compound was prepared as described for **6a**, from $AgClO_4$ (13 mg, 0.06 mmol), [AuCl(PCy$_3$)] (33 mg, 0.06 mmol), and (Pr$_4$N)[Pt{S$_2$C=(*t*-Bu-fy)}$_2$] (**2b**) (34 mg, 0.03 mmol). Yield: 42 mg, 71%. Anal. Calcd for $C_{80}H_{114}Au_2P_2PtS_4$: C, 51.80; H, 6.19; S, 6.91. Found: C, 52.10; H, 6.43; S, 7.27. mp: 180 °C (dec). IR (Nujol, cm^{-1}): ν(C=CS$_2$), 1538; ν(Pt−S), 346, 336. ^{1}H NMR (400.9 MHz, $CDCl_3$): δ 8.77 (d, $^4J_{HH}$ = 1.4 Hz, 4 H, H1, H8), 7.61 (d, $^3J_{HH}$ = 8.0 Hz, 4 H, H4, H5), 7.22 (dd, $^3J_{HH}$ = 8.0 Hz, $^4J_{HH}$ = 1.7 Hz, 4 H, H3, H6), 2.01−1.95 (br m, 18 H, Cy), 1.72−1.48 (br m, 30 H, Cy), 1.40 (s, 18 H, *t*-Bu), 1.17−1.12 (br m, 18 H, Cy). $^{13}C\{^1H\}$ (100.8 MHz, $CDCl_3$): δ 150.9 (CS_2), 148.7 (C2, C7), 138.4 (C8a, C9a), 135.3 (C4a, C4b), 133.5 (C9), 121.8 (C3, C6), 121.7 (C1, C8), 117.7 (C4, C5), 35.0 (*C*Me$_3$), 33.4 (d, $^1J_{CP}$ = 27.9 Hz, C1, Cy), 31.8 (C*Me$_3$*), 30.7 (C2, C6, Cy), 27.0 (d, $^3J_{CP}$ = 12.1 Hz, C3, C5, Cy), 25.7 (C4, Cy). $^{31}P\{^1H\}$ NMR (81.0 MHz, $CDCl_3$): δ 54.8.

[Pd{S$_2$C=(*t*-Bu-fy)}(dbbpy){Au(PCy$_3$)}]ClO$_4$·H$_2$O (5a). $AgClO_4$ (33 mg, 0.16 mmol) was added to a stirred suspension of [AuCl(PCy$_3$)] (80 mg, 0.16 mmol) in acetone (15 mL). After 10 min, the mixture was filtered through Celite to remove the precipitate of AgCl, and the clear filtrate was added to a suspension of complex **3a** (114 mg, 0.16 mmol) in acetone (10 mL). An immediate reaction was observed to give a turbid orange solution, which was stirred for 15 min, filtered through a PTFE syringe filter (0.45 μm pore size) to remove a small amount of insoluble material, and concentrated to ~8 mL. The addition of Et_2O (25 mL) led to the precipitation of an orange solid, which was filtered off, washed with acetone/Et_2O (1:2, 2 × 2 mL), and dried at 60 °C for 4 h to give **5a**. Yield: 180 mg, 87%. Anal. Calcd for $C_{58}H_{83}AuClN_2O_5PPdS_2$: C, 52.69; H, 6.33; N, 2.12; S, 4.85. Found: C, 52.87; H, 6.64; N, 2.15; S, 4.73. mp: 189 °C. IR (Nujol, cm^{-1}): ν(C=CS$_2$), 1564. ^{1}H NMR (400.9 MHz, CD_2Cl_2): δ 8.71 (d, $^4J_{HH}$ = 1.3 Hz, 2 H, H1, H8), 8.25 (d, $^4J_{HH}$ = 1.8 Hz, 2 H, H3, dbbpy), 8.15 (d, $^3J_{HH}$ = 5.8 Hz, 2 H, H6, dbbpy), 7.62 (dd, $^3J_{HH}$ = 5.8 Hz, $^4J_{HH}$ = 1.8 Hz, 2 H, H5, dbbpy), 7.48 (d, $^3J_{HH}$ = 7.9 Hz, 2 H, H4, H5), 7.25 (dd, $^3J_{HH}$ = 8.0 Hz, $^4J_{HH}$ = 1.7 Hz, 2 H, H3, H6), 1.84 (br m, 3 H, Cy), 1.67 (br m, 6 H, Cy), 1.55 (m, 9 H, Cy), 1.52 (s, 18 H, *t*-Bu, dbbpy), 1.48 (s, 18 H, *t*-Bu, dithiolato), 1.12 (br m, 12 H, Cy), 0.87 (br m, 3 H, Cy). $^{13}C\{^1H\}$ (100.8 MHz, CD_2Cl_2): δ 166.4 (C4, dbbpy), 155.1 (C2, dbbpy), 149.7 (C2, C7), 148.6 (C6, dbbpy), 146.4 (CS_2), 138.6 (C8a, C9a), 136.2 (C4a, C4b), 133.9 (C9), 124.8 (C5, dbbpy), 124.1 (C3, C6), 121.2 (C1, C8), 120.6 (C3, dbbpy), 118.8 (C4, C5), 36.4 (*C*Me$_3$, dbbpy), 35.3 (*C*Me$_3$, dithiolato), 33.3 (d, $^1J_{PC}$ = 28.5 Hz, C1, Cy), 31.9 (C*Me$_3$*, dithiolato), 31.1 (C2, Cy), 30.4 (C*Me$_3$*, dbbpy), 27.0 (d, $^3J_{PC}$ = 12.2 Hz, C3, Cy), 25.9 (C4, Cy). $^{31}P\{H\}$ NMR (162.3 MHz, CD_2Cl_2): δ 59.9.

[Pt{S$_2$C=(*t*-Bu-fy)}(dbbpy){Au(PCy$_3$)}]ClO$_4$·H$_2$O (5b). This complex was obtained as an orange solid following the procedure described for **5a**, from [AuCl(PCy$_3$)] (146 mg, 0.28 mmol), $AgClO_4$ (60 mg, 0.29 mmol), and [Pt{S$_2$C=(*t*-Bu-fy)}(dbbpy)] (**3b**) (230 mg, 0.28 mmol). Yield: 350 mg, 88%. Anal. Calcd for $C_{58}H_{83}AuClN_2O_5PPtS_2$: C, 49.37; H, 5.93; N, 1.99; S, 4.55. Found: C, 49.51; H, 6.19; N, 1.98; S, 4.30. mp: 90 °C (dec). IR (Nujol, cm^{-1}): ν(C=CS$_2$), 1572. ^{1}H NMR (400.9 MHz, CD_2Cl_2): δ 8.68 (d, $^4J_{HH}$ = 1.4 Hz, 2 H, H1, H8), 8.32 (d, $^3J_{HH}$ = 5.9 Hz, 2 H, H6, dbbpy), 8.26 (d, $^4J_{HH}$ = 1.4 Hz, 2 H, H3, dbbpy), 7.58 (dd, $^3J_{HH}$ = 5.9 Hz, $^4J_{HH}$ = 1.5 Hz, 2 H, H5, dbbpy), 7.45 (d, $^3J_{HH}$ = 7.9 Hz, 2 H, H4, H5), 7.20 (dd, $^3J_{HH}$ = 7.9 Hz, $^4J_{HH}$ = 1.7 Hz, 2 H, H3, H6), 1.79 (br m, 3 H, Cy), 1.64 (br m, 6 H, Cy), 1.53 (br m, 9 H, Cy), 1.50 (s, 18 H, *t*-Bu, dbbpy), 1.47 (s, 18 H, *t*-Bu, dithiolato), 1.09 (br m, 12 H, Cy), 0.85 (br m, 3 H, Cy). $^{13}C\{^1H\}$ (100.8 MHz, CD_2Cl_2): δ 166.0 (C4, dbbpy), 155.4 (C2, dbbpy), 149.7 (C2, C7), 147.8 (C6, dbbpy), 143.8 (CS_2), 138.1 (C8a, C9a), 136.3 (C4a, C4b), 135.9 (C9), 125.4 (C5, dbbpy), 124.1 (C3, C6), 121.2 (C1, C8, dithiolato + C3, dbbpy), 118.6 (C4, C5), 36.5 (*C*Me$_3$, dbbpy), 35.3 (*C*Me$_3$, dithiolato), 33.3 (d, $^1J_{PC}$ = 28.5 Hz, C1, Cy), 31.9 (C*Me$_3$*, dithiolato), 31.0 (C2, Cy), 30.3 (C*Me$_3$*, dbbpy), 27.0 (d, $^3J_{PC}$ = 12.2 Hz, C3, Cy), 25.9 (C4, Cy). $^{31}P\{H\}$ NMR (162.3 MHz, CD_2Cl_2): δ 57.6.

[Pd{S$_2$C=(*t*-Bu-fy)}(dbbpy){Au(PCy$_3$)}$_2$](ClO$_4$)$_2$ (6a). This complex was obtained as a yellowish orange microcrystalline solid, following the procedure described for **5a**, from [AuCl(PCy$_3$)] (163 mg, 0.32 mmol), $AgClO_4$ (70 mg, 0.34 mmol), and **3a** (113 mg, 0.16 mmol). Yield: 262 mg, 90%. Anal. Calcd for $C_{76}H_{114}Au_2Cl_2N_2O_8P_2PdS_2$: C, 48.53; H, 6.11; N, 1.49; S, 3.41. Found: C, 48.32; H, 6.41; N, 1.74; S, 3.22. mp: 169 °C (dec). IR (Nujol, cm^{-1}): ν(C=CS$_2$) not observed. ^{1}H NMR (400.9 MHz, CD_2Cl_2): δ 8.65 (d, $^4J_{HH}$ = 1.3 Hz, 2 H, H1, H8), 8.45 (d, $^3J_{HH}$ = 5.9 Hz, 2 H, H6, dbbpy), 8.40 (d, $^4J_{HH}$ = 1.2 Hz, 2 H, H3, dbbpy), 7.93 (dd, $^3J_{HH}$ = 5.7 Hz, $^4J_{HH}$ = 1.2 Hz, 2 H, H5, dbbpy), 7.65 (d, $^3J_{HH}$ = 8.0 Hz, 2 H, H4, H5), 7.47 (dd, $^3J_{HH}$ = 8.0 Hz, $^4J_{HH}$ = 1.5 Hz, 2 H, H3, H6), 1.99 (br m, 6 H, Cy), 1.77 (br m, 12 H, Cy), 1.61 (m, 18 H, Cy), 1.54 (s, 18 H, *t*-Bu, dbbpy), 1.48 (s, 18 H, *t*-Bu, dithiolato), 1.20 (br m, 24 H, Cy), 0.94 (m, 6 H, Cy). $^{13}C\{^1H\}$ NMR (100.8 MHz, CD_2Cl_2): δ 168.3 (C4, dbbpy), 155.6 (C2, dbbpy), 151.1 (C2, C7), 149.5 (C6, dbbpy), 142.5 (CS_2), 137.9 (C8a, C9a), 137.2 (C4a, C4b), 129.3 (C9), 127.0 (C3, C6), 125.9 (C5, dbbpy), 122.4 (C1, C8), 121.8 (C3, dbbpy), 119.7 (C4, C5), 36.9 (*C*Me$_3$, dbbpy), 35.4 (*C*Me$_3$, dithiolato), 33.4 (d, $^1J_{PC}$ = 29.0 Hz, C1, Cy), 31.8 (C*Me$_3$*, dithiolato), 31.3 (C2, Cy), 30.3 (C*Me$_3$*, dbbpy), 27.0 (d, $^3J_{PC}$ = 12.3 Hz, C3, Cy), 25.9 (d, $^4J_{PC}$ = 1.2 Hz, C4, Cy). $^{31}P\{^1H\}$ NMR (162.3 MHz, CD_2Cl_2): 61.5.

[Pt{S$_2$C=(*t*-Bu-fy)}(dbbpy){Au(PCy$_3$)}$_2$](ClO$_4$)$_2$ (6b). This complex was obtained as a yellow solid, following the procedure described for **5a**, from [AuCl(PCy$_3$)] (171 mg, 0.33 mmol), $AgClO_4$ (72 mg, 0.35 mmol), and **3b** (133 mg, 0.16 mmol). Yield: 211

Scheme 1 [a]

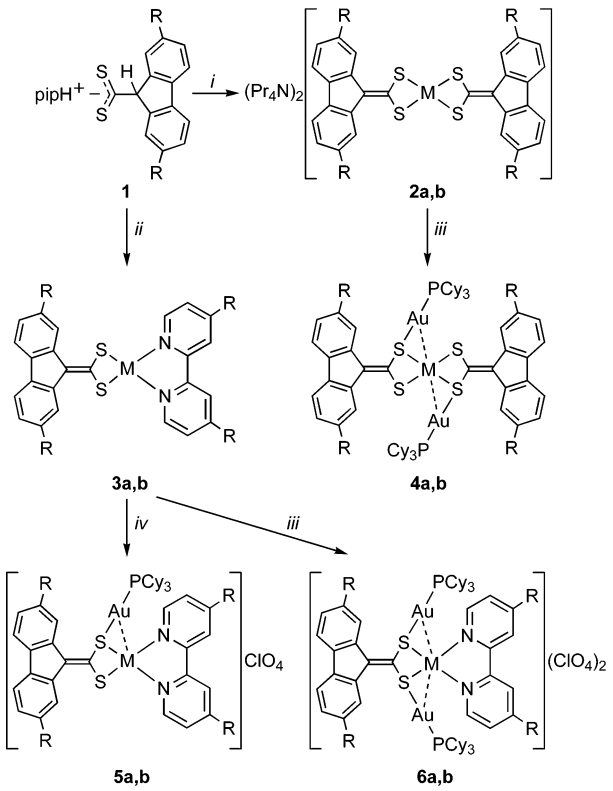

[a] M = Pd (**2**−**6a**), Pt (**2**−**6b**); R = *t*-Bu. (i) MCl_2, $(Pr_4N)Cl$, pip; (ii) $[MCl_2(dbbpy)]$, pip; (iii) $2[Au(OClO_3)(PCy_3)]$; (iv) $1[Au(OClO_3)(PCy_3)]$, where pip = piperidine and dbbpy = 4,4′-di-tert-butyl-2,2′-bipyridyl.

mg, 67%. Anal. Calcd for $C_{76}H_{114}Au_2Cl_2N_2O_8P_2PtS_2$: C, 46.34; H, 5.83; N, 1.42; S, 3.26. Found: C, 46.16; H, 6.00; N, 1.69; S, 3.02. mp: 180 °C. IR (Nujol, cm^{-1}): $\nu(C{=}CS_2)$ not observed. ^1H NMR (400.9 MHz, CD_2Cl_2): δ 8.65 (d, $^3J_{HH}$ = 6.0 Hz, 2 H, H6, dbbpy), 8.60 (d, $^4J_{HH}$ = 1.2 Hz, 2 H, H1, H8), 8.45 (d, $^4J_{HH}$ = 1.8 Hz, 2 H, H3, dbbpy), 7.93 (dd, $^3J_{HH}$ = 6.0 Hz, $^4J_{HH}$ = 1.9 Hz, 2 H, H5, dbbpy), 7.64 (d, $^3J_{HH}$ = 8.0 Hz, 2 H, H4, H5), 7.45 (dd, $^3J_{HH}$ = 8.0 Hz, $^4J_{HH}$ = 1.6 Hz, 2 H, H3, H6), 1.94 (br m, 6 H, Cy), 1.75 (br m, 12 H, Cy), 1.59 (br m, 18 H, Cy), 1.54 (s, 18 H, *t*-Bu, dbbpy), 1.47 (s, 18 H, *t*-Bu, dithiolato), 1.18 (br m, 24 H, Cy), 0.92 (br m, 6 H, Cy). $^{13}C\{^1H\}$ NMR (100.8 MHz, CD_2Cl_2): δ 168.2 (C4, dbbpy), 155.7 (C2, dbbpy), 151.2 (C2, C7), 148.9 (C6, dbbpy), 144.1 (CS_2), 138.0 (C8a, C9a), 136.6 (C4a, C4b), 134.8 (C9), 127.1 (C5, dbbpy), 126.5 (C3, C6), 122.3 (C1, C8, dithiolato + C3, dbbpy), 119.6 (C4, C5), 36.9 (*C*Me_3, dbbpy), 35.4 (*C*Me_3, dithiolato), 33.4 (d, $^1J_{PC}$ = 28.7 Hz, C1, Cy), 31.8 (C*Me*$_3$, dithiolato), 31.2 (C2, C6, Cy), 30.2 (C*Me*$_3$, dbbpy), 27.0 (d, $^3J_{PC}$ = 12.3 Hz, C3, C5 Cy), 25.9 (C4, Cy). $^{31}P\{^1H\}$ NMR (162.3 MHz, CD_2Cl_2): δ 59.5.

Results and Discussion

Syntheses. The mononuclear Pd(II) complexes with the (2,7-di-*tert*-butylfluoren-9-ylidene)methanedithiolato ligand can be prepared following the procedures described for the analogous Pt(II) complexes.[18] Thus, the anionic complex $(Pr_4N)_2[Pd\{S_2C{=}(t\text{-Bu-fy})\}_2]$ (**2a**) was obtained in moderate yield from the reaction of $PdCl_2$ with piperidine, Pr_4NCl, and piperidinium 2,7-di-*tert*-butyl-9*H*-fluorene-9-carbodithioate (**1**) in molar ratio of 1:2:2:2 in CH_2Cl_2 (Scheme 1). The addition of piperidine to CH_2Cl_2 suspensions of $PdCl_2$ results in the formation of clear solutions presumably containing *cis/trans*-$[PdCl_2(pip)_2]$. The dithioate **1** displaces the chloro and piperidine ligands and is then deprotonated by the free piperidine. The poorly soluble salt **2a** precipitated as an orange solid and was separated from the piperidinium chloride by washing with CH_2Cl_2. The neutral complex $[Pd\{S_2C{=}(t\text{-Bu-fy})(dbbpy)\]$ (**3a**, dbbpy = 4,4′-di-*tert*-butyl-2,2′-bipyridyl) was prepared in high yield by displacement of the chloro ligands in $[PtCl_2(dbbpy)]$ with dithioate **1** in the presence of piperidine.

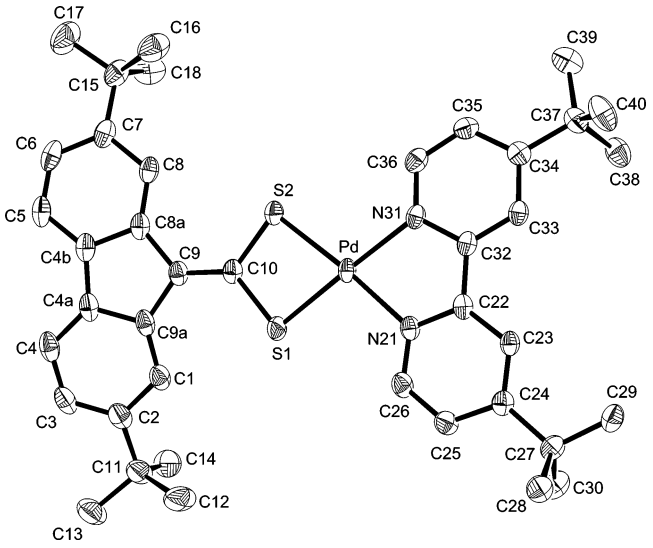

Figure 1. Thermal ellipsoid plot (50% probability) of complex **3a**. Hydrogen atoms are omitted for clarity.

The series of complexes $[M\{S_2C{=}(t\text{-Bu-fy})\}_2\{Au(PCy_3)\}_2]$ [M = Pd (**4a**), Pt (**4b**)], $[M\{S_2C{=}(t\text{-Bu-fy})\}(dbbpy)\{Au(PCy_3)\}]ClO_4$ [M = Pd (**5a**), Pt (**5b**)], and $[M\{S_2C{=}(t\text{-Bu-fy})\}(dbbpy)\{Au(PCy_3)\}_2](ClO_4)_2$ [M = Pd (**6a**), Pt (**6b**)] were prepared via the reaction of **2a** and **b** or **3a** and **b** with acetone solutions of $[Au(OClO_3)(PCy_3)]$, which in turn were generated from $[AuCl(PCy_3)]$ and $AgClO_4$ and used in situ in the appropriate molar ratios. The neutral complexes **4a** and **b** precipitated as yellow solids from the reaction mixtures and are remarkably stable compounds. The cationic complexes were crystallized from acetone/Et_2O as moderately stable orange (**5a**, **b**), yellowish orange (**6a**), or bright yellow (**6a**) solids. The monoaurated derivatives **5a** and **b** are stable in most common organic solvents, but they undergo appreciable dissociation of $[Au(PCy_3)]^+$ units in DMSO, PrCN, and DMF at concentrations below 10^{-4} M. The dissociation of $[Au(PCy_3)]^+$ units in solution is more favored for the diaurated compounds **6a** and **b** because of their dicationic nature and the diminished donating ability of **5a** and **b** relative to that of **3a** and **b**. Thus, although **6a** and **b** are stable in essentially non-coordinating solvents such as CH_2Cl_2 and $CHCl_3$, a significant dissociation of $[Au(PCy_3)]^+$ units to give **5a** and **b** takes place in all coordinating solvents and may be complete at concentrations below 10^{-4} M. These dissociation processes were revealed by the electronic absorption spectra and are discussed further below.

Crystal Structures of Complexes. The crystal structure of complex **3a** (Figure 1) was solved as a CH_2Cl_2 monosolvate. Selected bond distances and angles are listed in Table 2. The molecule exhibits the expected square planar coor-

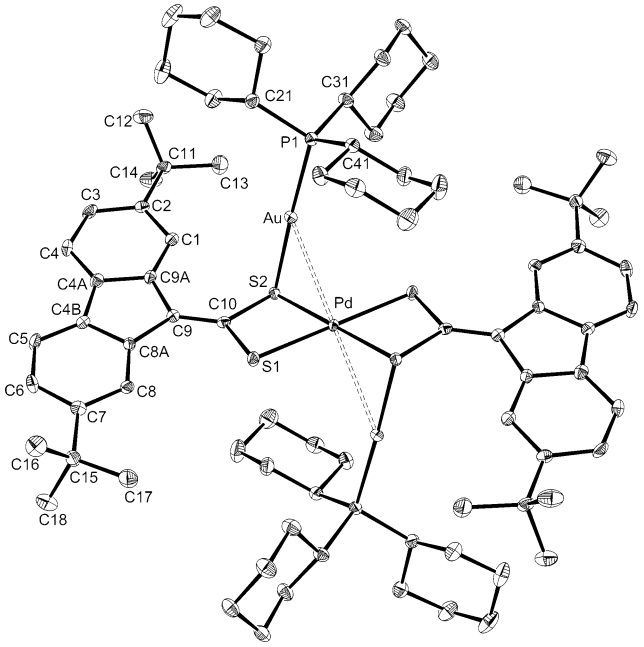

Figure 2. Thermal ellipsoid plot (50% probability) of the centrosymmetric molecular structure of complex **4a**. Hydrogen atoms are omitted for clarity.

Table 2. Selected Bond Distances (Å) and Angles (deg) for **3a**·CH_2Cl_2

Pd−N(21)	2.058(2)	S(1)−C(10)	1.753(3)
Pd−N(31)	2.079(2)	S(2)−C(10)	1.752(3)
Pd−S(1)	2.2562(8)	C(9)−C(10)	1.357(4)
Pd−S(2)	2.2738(7)		
N(21)−Pd−N(31)	78.50(9)	S(1)−Pd−S(2)	75.27(3)
N(21)−Pd−S(1)	100.79(6)	C(10)−S(1)−Pd	90.49(9)
N(31)−Pd−S(1)	176.17(6)	C(10)−S(2)−Pd	89.92(9)
N(21)−Pd−S(2)	175.47(6)	S(1)−C(10)−S(2)	104.23(14)
N(31)−Pd−S(2)	105.59(6)		

dination around the palladium atom (the mean deviation from plane S_2PdN_2 is 0.046 Å). The aromatic rings of the dbbpy ligand and the fluoren-9-ylidene moiety deviate significantly from the S_2PdN_2 mean plane [maximum deviations are found for the following: C(5), −0.94 Å; C(6), −0.81 Å; C(34), 0.58 Å; C(35), 0.48 Å], resulting in an appreciable bending of the whole molecule. The coordination geometry around the metal center is similar to that found for the related platinum complexes [Pt{S_2C═(MeO-fy)}(dbbpy)][18] (MeO-fy = 2,7-dimethoxyfluoren-9-ylidene), [Pt{S_2C═$(COMe)_2$}-(dbbpy)], and [Pt{S_2C═(CN)(C_6H_4Br-4}(dbbpy)].[22] The Pd−S and Pd−N bond distances are also comparable to the Pt−S and Pt−N distances found for the mentioned platinum homologs, as expected in view of the similar covalent radii of Pt and Pd.[26] As far as we are aware, this is the first reported crystal structure of a palladium 1,1-ethylenedithiolate diimine complex.

The X-ray single-crystal structure analyses of **4a** and **b** revealed that these complexes are isomorphous. The structure of **4a** is shown in Figure 2. Selected bond distances and angles for both complexes are listed in Table 3. The molecules exhibit crystallographic inversion symmetry, and therefore, the MS_4 cores are strictly planar. Both structures reveal very similar bond distances around the Pd and Pt

(26) Pauling, L. *J. Am. Chem. Soc.* **1947**, *69*, 542−553.

Table 3. Selected Bond Distances (Å) and Angles (deg) for **4a** and **4b**

	4a M = Pd	**4b** M = Pt
Au(1)−P(1)	2.2630(7)	2.2613(15)
Au(1)−S(2)	2.3316(7)	2.3386(14)
Au(1)−M	3.04793(14)	3.0529(2)
M−S(2)	2.3259(6)	2.3191(14)
M−S(1)	2.3282(7)	2.3276(15)
S(1)−C(10)	1.749(3)	1.753(6)
S(2)−C(10)	1.790(3)	1.790(6)
C(9)−C(10)	1.355(4)	1.353(7)
P(1)−Au(1)−S(2)	175.80(2)	175.16(5)
P(1)−Au(1)−M	131.494(18)	131.81(4)
S(2)−M−S(1)#1	105.06(2)	105.36(5)
S(2)−M−S(1)	74.94(2)	74.64(5)
S(1)#1−M−Au(1)	86.995(17)	87.42(4)
C(10)−S(1)−M	89.68(9)	90.1(2)
C(10)−S(2)−M	88.76(9)	89.51(19)
C(10)−S(2)−Au(1)	103.28(9)	103.31(18)
M−S(2)−Au(1)	81.75(2)	81.91(4)
S(1)−C(10)−S(2)	106.22(14)	105.4(3)

atoms, which is attributable to their almost equivalent covalent radii.[26] The coordination geometries around these atoms and the M−S bond distances are also very similar to those found in the crystal structures of $(Me_4N)_2$[Pd{S_2C═$(COMe)_2$}$_2$][13] and several salts of $[M(i\text{-mnt})_2]^{2-}$ (M = Pd,[12,27] Pt).[28] The fluoren-9-ylidene moieties are practically planar [main deviation from plane = 0.017 (**4a**), 0.019 (**4b**) Å] and rotated by 14.3° in both cases with respect to the S(1)−C(10)−S(2) plane. The gold atoms are bonded to one of the sulfur atoms of each dithiolato ligand and lie above and below the MS_4 plane. The arrangement of the gold atoms with respect to the MS_4 core is defined by the angles Au−S(2)−M of 81.75(2) (**4a**) or 81.91(4)° (**4b**) and the torsion angles Au−S(2)−M−S(1) of 107.70 (**4a**) or 107.31° (**4b**). The coordination around gold is almost linear, and the Au−S(2) distances of 2.3316(7) (**4a**) or 2.3386(14) Å (**4b**) are comparable to those found in the dinuclear complexes [{Au-(PR_3)}$_2${S_2C═(*t*-Bu-fy)}] (R = Me, Ph) and [{Au(PPh_3)}$_2${S_2C═(fy)}][16] or the mononuclear complexes [Au{SC(═S)NEt_2}(PCy_3)] and [Au{SC(═S)OR}(PCy_3)] (R = Ph, Pr, *i*-Pr, Et),[29] all of which feature $[Au(PR_3)]^+$ units bonded to nonbridging thiolate functions. Despite the apparent strength of the Au−S bonds, the coordination of $[Au(PCy_3)]^+$ units to the $[M\{S_2C{=}(t\text{-Bu-fy})\}_2]^{2-}$ anions does not have a significant influence on the bond distances and angles in the MS_4 core and causes only a slight lengthening of the C(10)−S(2) bond distance [1.790(3) (**4a**), 1.790(6) Å (**4b**)] as compared to C(10)−S(1) [1.749(3) (**4a**), 1.753(6) Å (**4b**)], which is attributable to a decrease in the bond order. There are Au···M contacts of 3.0479(1) (**4a**) and 3.0529(2) Å (**4b**), which are shorter than the sum of van der Waals radii for Au and Pd (3.29 Å) or Pt (3.38 Å)[30] and lie in the range

(27) (a) Cao, R.; Su, W.; Hong, M.; Tatsumi, K. *Chem. Lett.* **1999**, 1219−1220. (b) Long, D. L.; Hou, H. W.; Xin, X. Q.; Yu, K. B.; Luo, B. S.; Chen, L. R. *J. Coord. Chem.* **1996**, *38*, 15.

(28) (a) Hummel, H. U. *Trans. Met. Chem.* **1987**, *12*, 172−174. (b) Gao, X.-M.; Dou, J.-M.; Li, D.-C.; Dong, F.-Y.; Wang, D.-Q. *J. Mol. Struct.* **2005**, *733*, 181−186.

(29) (a) Siasios, G.; Tiekink, E. R. T. *Z. Kristallogr.* **1993**, *205*, 261−270. (b) Siasios, G.; Tiekink, E. R. T. *Z. Kristallogr.* **1993**, *203*, 117−119.

(30) Bondi, A. *J. Phys. Chem.* **1964**, *68*, 441−451.

expected for d^8-d^{10} metallophilic interactions.[6,31] We note that only five crystal structures in the Cambridge Structural Database[32] display weak Pd···Au contacts of similar length, namely, those of $[\{Pd(SeH)(PPh_3)\}_2\{Au(PPh_3)\}_2(\mu_3\text{-}Se)_2]$ (3.067 Å),[33] $[PdCl_2\{AuCl(PPh_2CH_2SPh)\}_2]$ (3.142 Å),[34] $[\{Pd(CN)_2\}Au(\mu\text{-dcpm})_2]$ [2.954 Å; dcpm = bis(dicyclohexylphosphino)methane],[31] $[\{Pd(dbbpy)\}_2\{Au(PPh_3)\}_2(\mu_3\text{-}O)_2]$ (2.985 Å), and $[\{Pd(dbbpy)\}_4\{Au(PPh_3)\}_2(\mu_3\text{-}O)_3](BF_4)_3$ (3.071, 3.065, 3.211 Å),[35] while five other structures exhibit Pd···Au distances in the range of 3.300−3.500 Å.[36] Complexes with weak Pt···Au contacts are more numerous[3,31,37] and include the tetranuclear complex $[\{Pt(PPh_3)_2\}_2Au_2\{S_2C{=}(COMe)_2\}_2](ClO_4)_2$ (3.224, 3.334 Å),[14] the trinuclear ylide complex $[Au_2Pt\{CH_2P(S)Ph_2\}]$ (3.034 Å),[38] and several complexes with bridging sulfido ligands (range of 3.016−3.495 Å).[39] The 1,2-dithiolene complex $[Pt(mnt)_2\{Au(PPh_3)\}_2]$[40] (mnt = maleonitriledithiolate) is the closest structural relative to complexes **4a** and **b** and also exhibits inversion symmetry and similarly situated $[Au(PPh_3)]^+$ units, but with a wider Au−S−Pt angle of 95.45° leading to an appreciably longer Au···Pt distance of 3.415 Å.

The structure of complex **5b** (Figure 3) was solved as an acetone monosolvate. Selected bond distances and angles are listed in Table 4. The essentially planar $[Pt\{S_2C{=}(t\text{-Bu-fy})\}(dbbpy)]$ unit (mean deviation of 0.075 Å, excluding the *t*-Bu groups) is coordinated to a $[Au(PCy_3)]^+$ unit through one of the sulfur atoms of the dithiolato ligand. The Au−S(1) distance and the arrangement of the $[Au(PCy_3)]^+$ unit relative to the $[Pt\{S_2C{=}(t\text{-Bu-fy})\}(dbbpy)]$ complex are similar to those found in **4a** and **b**, with the torsion angle Au(1)−S(1)−Pt(1)−S(2) of 107.66° being almost identical to its counterparts in **4a** and **b**. However, the Au(1)−S(1)−Pt(1) angle of 91.92(2)° is appreciably wider and leads to a longer Au···Pt contact of 3.3108(2) Å. The Pt−S(1) bond distance [2.2683(6) Å] is slightly shorter than Pt−S(2) [2.2835(6) Å], but they are not significantly different from the Pt−S distances found in $[Pt\{S_2C{=}(MeO\text{-fy})\}(dbbpy)]$.[18] As for

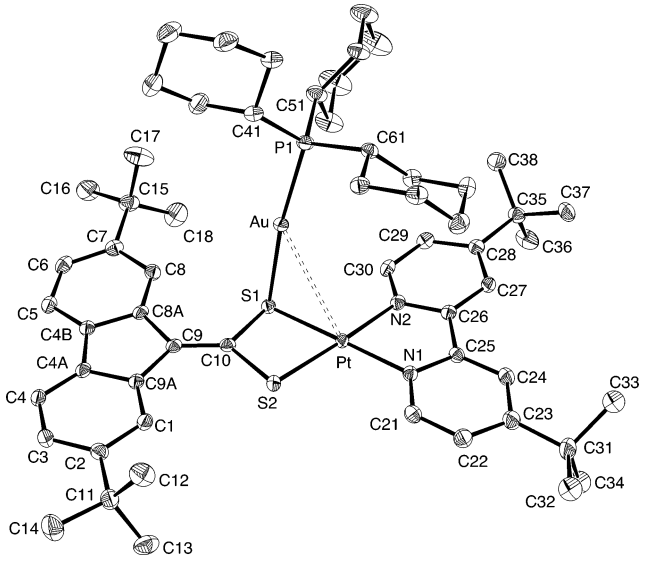

Figure 3. Thermal ellipsoid plot (50% probability) of the cation of complex **5b**. Hydrogen atoms are omitted for clarity.

Table 4. Selected Bond Distances (Å) and Angles (deg) for **5b**·Me_2CO

Au(1)−Pt(1)	3.31076(17)	Pt(1)−S(1)	2.2683(6)
Au(1)−P(1)	2.2735(6)	Pt(1)−S(2)	2.2835(6)
Au(1)−S(1)	2.3367(6)	S(1)−C(10)	1.794(2)
Pt(1)−N(1)	2.035(2)	S(2)−C(10)	1.755(2)
Pt(1)−N(2)	2.035(2)	C(9)−C(10)	1.347(3)
P(1)−Au(1)−S(1)	172.32(2)	S(1)−Pt(1)−S(2)	75.86(2)
P(1)−Au(1)−Pt(1)	131.340(17)	C(10)−S(1)−Pt(1)	89.76(8)
N(1)−Pt(1)−N(2)	79.47(8)	C(10)−S(1)−Au(1)	106.06(8)
N(1)−Pt(1)−S(1)	179.32(6)	Pt(1)−S(1)−Au(1)	91.92(2)
N(2)−Pt(1)−S(1)	101.11(6)	C(10)−S(2)−Pt(1)	90.25(8)
N(1)−Pt(1)−S(2)	103.57(6)	S(2)−C(10)−S(1)	104.08(12)
N(2)−Pt(1)−S(2)	176.96(6)		

4a and **b**, the coordination of a $[Au(PCy_3)]^+$ unit to one of the sulfur atoms of the dithiolato ligand causes a lengthening of the corresponding C−S distance [C(10)−S(1) = 1.794(2) Å] relative to the other one [C(10)−S(2) = 1.755(2) Å]. The cations of **5b** stack in pairs, related by an inversion center (Figure 4). The distance between the mean planes of two adjacent $[Pt\{S_2C{=}(t\text{-Bu-fy})\}(dbbpy)]$ units is 3.44 Å, which is typical for π-stacked planar molecules,[16,41] and the closest contacts are found between atoms C(10) and S(1) (3.462 Å) and between C(25) and C(5) (3.340 Å).

Complex **6a** crystallized with one molecule each of THF and hexane in the asymmetric unit. The molecular structure of the dication is shown in Figure 5, and selected bond distances and angles are given in Table 5. The structure is composed of one $[Pd\{S_2C{=}(t\text{-Bu-fy})\}(dbbpy)]$ unit with two $[Au(PCy_3)]^+$ units bonded to the sulfur atoms of the dithiolato ligand. The Au(1)−S(1) and Au(2)−S(2) bond distances of 2.3452(9) and 2.3345(9) Å, respectively, compare well to those found for **4a**, and the torsion angles Au(1)−S(1)-Pd−S(2) and Au(2)−S(2)-Pd−S(1) of 97.38 or 99.25°, respectively, are slightly narrower. The Au(1)−S(1)−Pd angle of 82.94(3)° is similar to the corresponding one in **4a** and leads to a comparably short Pd···Au(1) contact of 3.0658(3) Å,

(31) Xia, B. H.; Zhang, H. X.; Che, C. M.; Leung, K. H.; Phillips, D. L.; Zhu, N. Y.; Zhou, Z. Y. *J. Am. Chem. Soc.* **2003**, *125*, 10362−10374.
(32) Allen, F. H. *Acta Crystallogr., Sect. B: Struct. Sci.* **2002**, *58*, 380−388.
(33) Harvey, P. D.; Eichhöfer, A.; Fenske, D. *J. Chem. Soc., Dalton Trans.* **1998**, 3901−3903.
(34) Crespo, O.; Laguna, A.; Fernández, E. J.; López-de-Luzuriaga, J. M.; Jones, P. G.; Teichert, M.; Monge, M.; Pyykkö, P.; Runeberg, N.; Schütz, M.; Werner, H. J. *Inorg. Chem.* **2000**, *39*, 4786−4792.
(35) Singh, A.; Sharp, P. R. *Dalton Trans.* **2005**, 2080−2081.
(36) (a) Balch, A. L.; Fung, E. Y.; Olmstead, M. M. *Inorg. Chem.* **1990**, *29*, 3203−3207. (b) Chiffey, A. F.; Evans, J.; Levason, W.; Webster, M. *Polyhedron* **1996**, *15*, 591−596. (c) Forniés, J.; Martín, A.; Sicilia, V.; Martín, L. F. *Chem.—Eur. J.* **2003**, *9*, 3427−3435.
(37) (a) Manojlović-Muir, L.; Henderson, A. N.; Treurnicht, I.; Puddephatt, R. J. *Organometallics* **1989**, *8*, 2055−2061. (b) Xu, C. F.; Anderson, G. K.; Brammer, L.; Braddock-Wilking, J.; Rath, N. P. *Organometallics* **1996**, *15*, 3972−3979.
(38) Murray, H. H.; Briggs, D. A.; Garzón, G.; Raptis, R. G.; Porter, L. C.; Fackler, J. P., Jr. *Organometallics* **1987**, *6*, 1992−1995.
(39) (a) Li, Z. H.; Loh, Z. H.; Mok, K. F.; Hor, T. S. A. *Inorg. Chem.* **2000**, *39*, 5299−5305. (b) Hallam, M. F.; Luke, M. A.; Mingos, D. M. P.; Williams, I. D. *J. Organomet. Chem.* **1987**, *325*, 271−283. (c) Bos, W.; Bour, J. J.; Schlebos, P. P. J.; Hageman, P.; Bosman, W. P.; Smits, J. M. M.; Vanwietmarschen, J. A. C.; Beurskens, P. T. *Inorg. Chim. Acta* **1986**, *119*, 141−148.
(40) Fritsch, E.; Polborn, K.; Robl, C.; Sünkel, K.; Beck, W. *Z. Anorg. Allg. Chem.* **1993**, *619*, 2050−2060.
(41) (a) Smucker, B. W.; Hudson, J. M.; Omary, M. A.; Dunbar, K. R. *Inorg. Chem.* **2003**, *42*, 4714−4723. (b) Ionkin, A. S.; Marshall, W. J.; Wang, Y. *Organometallics* **2005**, *24*, 619−627.

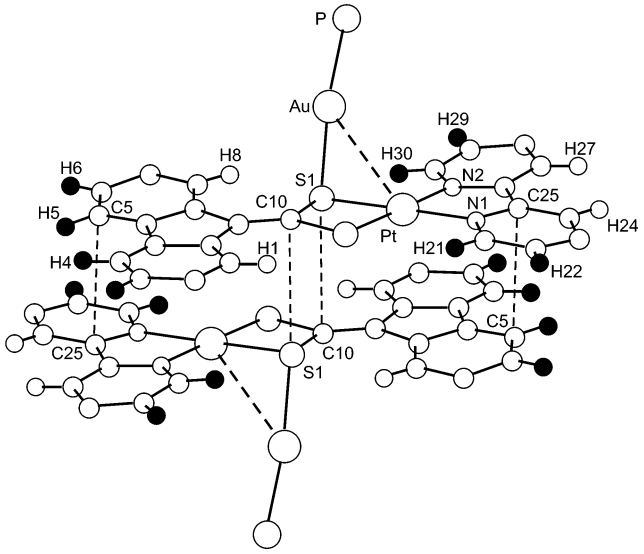

Figure 4. Stacked dimer in the structure of **5b**. The shortest contacts are highlighted by dashed lines. *t*-Bu and Cy groups are omitted for clarity. Hydrogen atoms in black are significantly shielded upon stacking in solution because of the magnetic anisotropy effect of the adjacent aromatic rings.

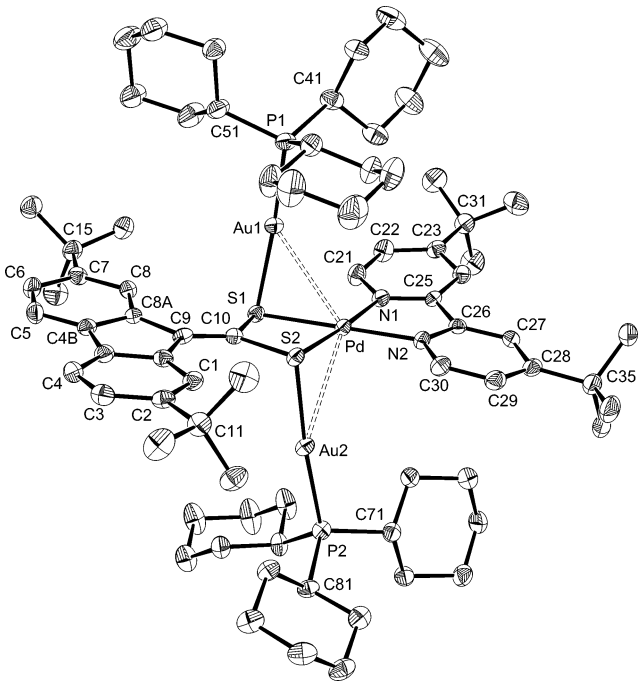

Figure 5. Thermal ellipsoid plot (50% probability) of the cation of complex **6a**. Hydrogen atoms are omitted for clarity.

while the wider Au(2)−S(2)−Pd angle of 90.01(3)° compares to the value found for Au−S(1)−Pt in **5b** and leads to a longer Pd···Au(2) contact of 3.2670(3) Å. As expected in view of the previous structures, the C(10)−S(1) and C(10)−S(2) bond distances of 1.784(4) and 1.785(4) Å are somewhat longer than the corresponding distances in **3a**, while the lengthening of the Pd−S(1) and Pd−S(2) distances [2.2839(10) and 2.2851(9) Å] relative to **3a** is less important.

NMR Spectra and Dynamic Behavior. The ^{1}H and ^{13}C NMR spectra of the Pd complexes **2a** and **3a** are very similar to those of their Pt counterparts[18] and agree with the proposed structures (see Experimental Section). The chemical shifts of the H1 and H8 protons (δ 8.97−8.40) are considerably higher than those in the free dithioate **1**, which is generally observed for coordinated (fluoren-9-ylidene)methanedithiolato ligands.[16−18]

Table 5. Selected Bond Distances (Å) and Angles (deg) for **6a**·THF·C_6H_{14}

Au(1)−P(1)	2.2543(10)	Pd(1)−N(1)	2.050(3)
Au(1)−S(1)	2.3452(9)	Pd(1)−S(1)	2.2839(10)
Au(1)−Pd(1)	3.0658(3)	Pd(1)−S(2)	2.2851(9)
Au(2)−P(2)	2.2714(10)	S(1)−C(10)	1.784(4)
Au(2)−S(2)	2.3345(9)	S(2)−C(10)	1.785(4)
Au(2)−Pd(1)	3.2670(3)	C(9)−C(10)	1.339(5)
Pd(1)−N(2)	2.047(3)		
P(1)−Au(1)−S(1)	171.51(3)	N(2)−Pd(1)−Au(2)	92.62(9)
P(1)−Au(1)−Pd(1)	132.92(3)	N(1)−Pd(1)−Au(2)	137.41(8)
P(2)−Au(2)−S(2)	174.94(3)	Au(1)−Pd(1)−Au(2)	124.413(10)
P(2)−Au(2)−Pd(1)	131.76(3)	C(10)−S(1)−Pd(1)	89.46(12)
N(2)−Pd(1)−N(1)	79.30(12)	C(10)−S(1)−Au(1)	94.41(12)
N(2)−Pd(1)−S(1)	179.11(9)	Pd(1)−S(1)−Au(1)	82.94(3)
N(1)−Pd(1)−S(1)	101.54(9)	C(10)−S(2)−Pd(1)	89.39(12)
N(2)−Pd(1)−S(2)	102.78(9)	C(10)−S(2)−Au(2)	102.11(12)
N(1)−Pd(1)−S(2)	176.56(9)	Pd(1)−S(2)−Au(2)	90.01(3)
S(1)−Pd(1)−S(2)	76.36(3)	S(1)−C(10)−S(2)	104.61(19)

The dithiolato ligands in the Pd/Au and Pt/Au complexes **4a** and **b** and **5a** and **b** give rise to only three resonances for the aromatic protons H1/H8, H3/H6, and H4/H5 and one resonance for the *t*-Bu groups in the ^{1}H NMR spectra, while the coordination of one of the sulfur atoms to a $[Au(PCy_3)]^+$ unit should make all the aromatic protons and the *t*-Bu groups inequivalent. This suggests the existence of dynamic processes in solution, which were studied by variable-temperature ^{1}H NMR measurements and are discussed below. In addition, the ^{1}H NMR spectra of the dinuclear complexes **5a** and **b** are concentration dependent and show that the resonances of all the aromatic protons except H1/H8 (dithiolate) and H3 (dbbpy) shift to lower frequencies with increasing concentration. The ^{1}H NMR spectra of the Pt complex **5b** at different concentrations in the range from 2.2 $\times$ 10^{-2} to 7.4 $\times$ 10^{-4} M are shown in Figure 6; the H6 protons of the dbbpy ligand are the most affected ($\Delta\delta$ = 0.23 ppm in the studied concentration range), followed by the H4/H5 and H3/H6 protons of the dithiolate and the H5 protons of the diimine. Similar variations in the chemical shifts of these protons are observed for the Pd complex **5a** (see Supporting Information). These observations are consistent with the formation of π-stacked dimers in solution, which affects the chemical shifts of some of the aromatic protons because of the magnetic anisotropy of adjacent aromatic rings. Thus, if the dimers in solution are assumed

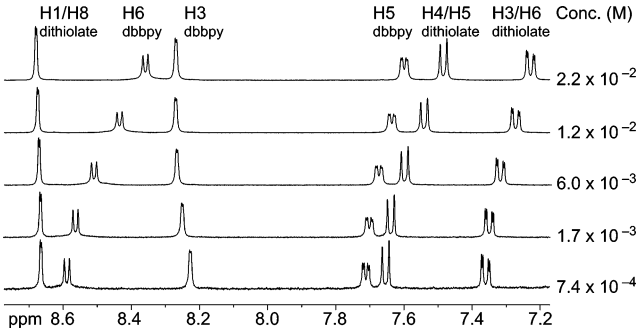

Figure 6. Room-temperature ^{1}H NMR spectra of **5b** in CD_2Cl_2 (400.9 MHz) at different concentrations (aromatic region).

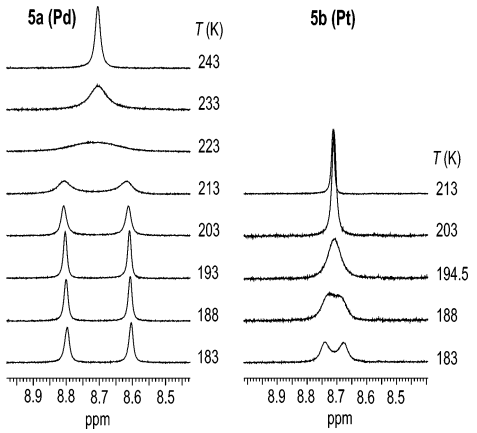

Figure 7. Variable-temperature ^{1}H NMR spectra of complexes **5a** and **b** in CD_2Cl_2 (400.9 MHz; H1 and H8 resonances).

to have essentially the structure found for **5b** in the solid state (Figure 4), the H6 and H5 atoms of the dbbpy ligand (labeled as H30/H21 and H29/H22, respectively, in the crystal structure of **5b**) should be shielded upon stacking in solution because they are located over the shielding region of the fluoren-9-ylidene moiety of the adjacent cation, while the H3 atoms (labeled as H27/H24) lie further apart and should not be affected. Similarly, the H3/H6 and H4/H5 atoms of the fluoren-9-ylidene groups are located over the shielding region of the dbbpy ligand of the adjacent cation, while the H1/H8 atoms lie well outside. Therefore, the increase of the fraction of π-stacked dimers with concentration explains the gradual shielding of all the aromatic protons except H1/H8 (dithiolate) and H3 (dbbpy).

The existence of a dynamic process involving the migration of the $[Au(PCy_3)]^+$ units between the sulfur atoms of the dithiolato ligands can be clearly confirmed for the simplest cases **5a** and **b** by means of variable-temperature ^{1}H NMR analyses. The ^{1}H NMR spectrum of the Pd complex **5a** at 183 K in CD_2Cl_2 shows two resonances for the H1 and H8 protons of the dithiolato ligand at δ 8.80 and 8.60, which coalesce at 223 K and at 293 K and give rise to one resonance at δ 8.71 (Figure 7). The resonance of the *t*-Bu groups of the dithiolato ligand in **5a** also splits at 183 K into two broad singlets at δ 1.45 and 1.41, which coalesce at 203 K, while the resonance arising from the *t*-Bu groups of dbbpy does not split. In the case of the Pt complex **5b**, only the resonances corresponding to the H1 and H8 protons split at 183 K, appearing as broad signals at δ 8.69 and 8.63 in CD_2Cl_2 and coalescing at 188 K. The resonances of the H3/H6 and H4/H5 atoms of the dithiolato ligand and those of H5 and H6 of the dbbpy ligand broaden and move to lower frequencies upon cooling to 183 K and only that of H5 (dbbpy) in **5a** splits into two broad signals (see Supporting Information for further details); the shielding of these protons can be attributed to an increasing fraction of π-stacked dimers.

The Arrhenius and Eyring activation parameters corresponding to the exchange processes in **5a** and **b** can be obtained by means of line-shape analysis of the temperature-dependent H1/H8 resonances and are listed in Table 6. The coalescence temperature and activation enthalpy are significantly higher for the Pd complex **5a** than for its Pt counterpart **5b** and are also associated with a larger splitting of the H1/H8 resonances for the Pd complex (0.20 ppm for **5a** vs 0.06 ppm for **5b**). It is reasonable to propose that the migration of the $[Au(PCy_3)]^+$ unit takes place through a symmetrical transition state, in which the metallophilic M···Au contact strengthens as the Au−S bond cleaves and a new Au−S bond begins to form (Scheme 2). The M···Au interaction could thus assist the migration process by lowering the energy of such a transition state. The higher enthalpy of activation for **5a** as compared to **5b** would then be the consequence of Pd···Au contacts being weaker, that is, having a lower interaction energy, than the Pt···Au contacts. Additionally, the stronger Pt···Au interaction in **5b** could be connected with a weaker effect of the $[Au(PCy_3)]^+$ unit on the H1/H8 atoms and therefore a smaller splitting of their resonances. The entropy of activation is close to zero for the Pd complex **5a**, which is typical for unimolecular processes. However, the more negative $\Delta S^{\ddagger}$ value found for the Pt complex **5b** does not have a clear explanation; the participation of the perchlorate anion in the formation of the transition state is one possible cause.

Table 6. Arrhenius and Eyring Activation Parameters for the Exchange Processes in **5a,b**

compd	E_A (kcal mol^{-1})	$\Delta H^{\ddagger}$ (kcal mol^{-1})	$\Delta S^{\ddagger}$ (cal mol^{-1} K^{-1})	T_{coal} (K)	$\Delta G^{\ddagger}_{coal}$ (kcal mol^{-1})
5a	10.6 ± 0.6	10.1 ± 0.6	-2 ± 2	223	10.7 ± 0.2
5b	7.4 ± 1.1	7.1 ± 0.5	-12 ± 2	188	9.3 ± 0.1

Scheme 2

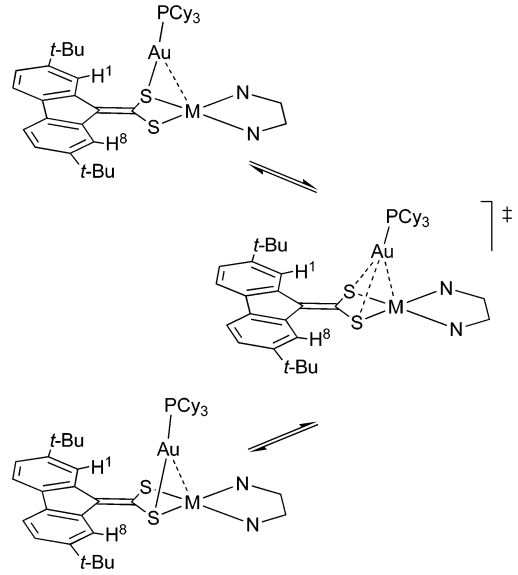

The variable-temperature ^{1}H NMR and ^{31}P NMR spectra of **4a** also confirmed the existence of a dynamic process. In this case, however, the migration of the $[Au(PCy_3)]^+$ units between the sulfur atoms can lead to three different isomers, labeled as **A**, **B**, and **C** in Scheme 3. At 183 K, the ^{1}H NMR spectrum shows that only the resonances of the H1 and H8 protons split, giving three broad signals at δ 8.87, 8.82, and 8.68 with relative intensities of 0.7:1.2:2.0, which coalesce at 203 K (Figure 8), while the ^{31}P NMR spectrum shows two broad signals at δ 57.4 and 57.3 with relative intensities

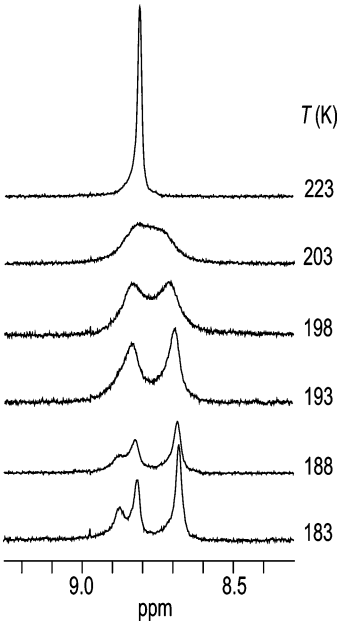

Figure 8. Variable-temperature ^{1}H NMR spectra of complex **4a** in CD_2Cl_2 (400.9 MHz; H1 and H8 resonances).

Scheme 3

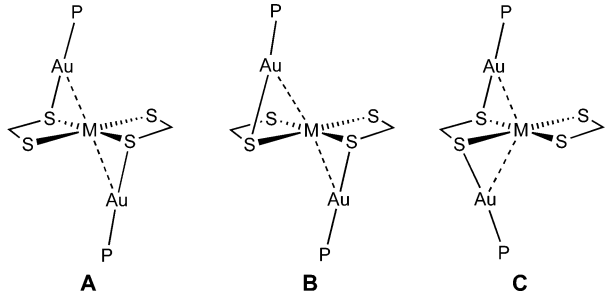

of 1:1.5, which coalesce at 188 K. These data suggest the presence of two different isomers with inequivalent H1 and H8 protons in different concentrations, although it is likely that the three possible isomers are indeed present and that two of them (**A** and **B**) give rise to almost co-incident ^{1}H and ^{31}P resonances that do not resolve at 183 K. In the case of the Pt complex **4b**, no splitting of the H1/H8 or phosphorus resonances was observed at 183 K, probably because of a much lower coalescence temperature. Although the variable-temperature NMR data of **4a** and **b** did not allow us to determine any activation parameters, the lower coalescence temperatures compared to those of **5a** and **b** are indicative of higher rate constants and lower enthalpies of activation. If we assume a transition state similar to that proposed for **5a** and **b**, this observation is consistent with stronger M···Au contacts in **4a** and **b** than in **5a** and **b**, which are expected because of the dianionic nature of the mononuclear precursors **2a** and **b** and the higher Coulombic contribution to these interactions.[5] Analogous reasoning leads to the conclusion that the Pd···Au contacts in **4a** must be weaker than the Pt···Au contacts in **4b**, which is in agreement with the differences observed between **5a** and **b**. As far as we are aware, there are no systematic studies that would permit a direct comparison of the interaction energies for Pd···Au and Pt···Au contacts. However, it is usually accepted that metallophilic interactions between heavier elements are stronger because of increasing contributions from relativistic effects.[6,42] In connection with this, we note that recent calculations on the model *trans*-$H_2Pd(PH_3)_2$···$HAuPH_3$ yielded an interaction energy of 8.4 kcal mol^{-1} for the Pd···Au contact (LMP2),[34] while in *trans*-$Pt(PH_3)_2(CN)_2$···$Au(PH_3)_2^+$, the Pt···Au interaction energy is 10.4 kcal mol^{-1} (MP2).[31]

The trinuclear complexes **6a** and **b** are also expected to undergo a similar dynamic process leading to the interchange of the $[Au(PCy_3)]^+$ units between the sulfur atoms. However, the dithiolato ligand in these molecules does not have inequivalent H1 and H8 protons or *t*-Bu groups, and therefore, their dynamic behavior cannot be verified by means of variable temperature NMR measurements.

IR Spectra. The solid-state IR spectra of mononuclear Pd complexes **2a** and **3a** show one band at 1500 or 1536 cm^{-1}, respectively, assignable to the ν(C═CS_2) mode.[43] These energies are identical to those found for the corresponding Pt counterparts **2b** and **3b**.[18] We have previously shown that the energy of the ν(C═CS_2) band in complexes with (fluoren-9-ylidene)methanedithiolate and its substituted derivatives is sensitive to variations in the electron-accepting ability of the metal center.[16,18] Usually, a higher oxidation state or the presence of weaker donor ligands strengthens the π component of the C═CS_2 double bond, thereby increasing the energy of the corresponding stretching vibration. This is consistent with the fact that the energy of the ν(C═CS_2) band for the anionic complexes **2a** and **b** is lower than for the neutral diimine complexes **3a** and **b**. The replacement of Pt by Pd does not have an effect on the energy of this band, consistent with the very similar acceptor character of these metals.

The energy of the ν(C═CS_2) band increases significantly on going from **2a** and **b** to the trinuclear **4a** and **b** complexes (1538 cm^{-1} in both cases) because the coordinated $[Au(PCy_3)]^+$ units withdraw additional electron density from the dithiolato ligands. Similarly, the cationic complexes **5a** and **b** display higher energies for this band (1564 or 1572 cm^{-1}, respectively) than their mononuclear precursors **3a** and **b**. However, the ν(C═CS_2) band was not observed in the IR spectra of the trinuclear complexes **6a** and **b**.

Bands arising from ν(M−S) modes were observed only for **2a** and **4a** and **b**. In the case of **2a**, the ν(Pd−S) band appears at 342 cm^{-1}, which is slightly higher in energy than the ν(Pt−S) band arising from **2b** at 338 cm^{-1}.[18] For the trinuclear complexes, two bands are observed at 354 and 334 cm^{-1} (**4a**) or 346 and 336 cm^{-1} (**4b**).

Electronic Absorption Spectra. The UV−vis absorption spectra were measured in CH_2Cl_2 at 298 K. The absorptions with λ > 330 nm are listed in Table 7. The intense lowest-energy absorption band observed for **2a** at 459 nm can be assigned to a metal-to-ligand charge-transfer (MLCT) transition from the mixed Pd(d)/$\pi_{dithiolate}$ HOMO and a dithiolate-based π* orbital.[19,44] Its large molar extinction coefficient is

(42) Pyykkö, P. *Angew. Chem., Int. Ed.* **2004**, *43*, 4412−4456.
(43) Jensen, K. A.; Henriksen, L. *Acta Chem. Scand.* **1968**, *22*, 1107−1128.
(44) Werden, B. G.; Billig, E.; Gray, H. B. *Inorg. Chem.* **1966**, *5*, 78−81.

Table 7. Electronic Absorption Data for Compounds **2-6a,b** in CH_2Cl_2 Solution (*ca.* 5×10^{-5} M) at 298 K ($\lambda > 330$ nm)

compd	λ/nm (ϵ/M^{-1} cm^{-1})
2a	345 (35 800), 407 (15 000), 435 (sh, 40 800), 459 (100 800)
2b	337 (28 100), 428 (12 200), 490 (57 600)
3a	375 (32 800), 391 (36 000), 467 (5700)
3b	381 (27 800), 397 (31 400), 543 (10 000)
4a	412 (sh, 43 400), 432 (60 800)
4b	437 (sh, 33 300), 470 (49 600)
5a	359 (25 800), 376 (30 400), 431 (5700)
5b	379 (27 900), 494 (8500)
6a	341 (23 400), 353 (24 900)
6b	343 (sh, 19 500), 356 (21 300), 397 (sh, 8200)

typical of charge-transfer transitions in 1,1-ethylenedithiolato complexes.[45] The significantly higher energy of this band for the Pd complex **2a** than for its Pt analog **2b** (490 nm)[18] is characteristic of MLCT transitions involving these metals.[44,46] When compared with $[Pd(i\text{-mnt})_2]^{2-}$ (377 nm),[44] the energy of the MLCT transition in **2a** is much lower because of the higher electron-donating ability of the (2,7-di-*tert*-butylfluoren-9-ylidene)methanedithiolato ligand, which raises the energy of the HOMO and therefore decreases the HOMO−LUMO energy gap. In contrast, the analogous complex with the closely related (cyclopentadienylidene)-methanedithiolato ligand displays a similar energy for this band (469 nm).[47]

The absorption spectra of complexes **4a** and **b** show one relatively broad band at 432 and 470 nm, respectively, with a shoulder on the higher-energy slope (412 or 437 nm). The corresponding molar extinction coefficients are high, but they are significantly lower than those of the lowest absorption band of **2a** and **b**. The higher energy of this band for the Pd relative to the Pt complex is indicative of metal orbital involvement. Its most probable origin is an MLCT transition of similar orbital parentage to that observed for the anionic complexes **2a** and **b**; its higher energy can be reasonably explained by the effect of the coordination of each dithiolato ligand to one $[Au(PCy_3)]^+$ unit, which necessarily causes a significant decrease in the energy of the sulfur orbitals and hence of the mixed metal/dithiolate HOMO, thereby raising the HOMO−LUMO energy gap.

The absorption spectrum of the diimine complex **3a** in CH_2Cl_2 (Figure 9) has basically the same profile as that of its Pt analog **3b**.[18] The two intense bands at 374 and 391 nm are insensitive to variations in solvent polarity and can be assigned to dithiolate-based transitions, while the broad lowest-energy absorption band at 496 nm is strongly solvent-dependent and corresponds to the charge transfer to diimine transition typically observed for Pd(II) and Pt(II) diimine dithiolates.[23,46] The UV−vis spectra of **3a** in a variety of organic solvents showed that this band shifts to lower energy as solvent polarity decreases (Table 8). The plot of this energy against the Pt(NN)(SS) solvent parameter[23] gave a good linear correlation ($R^2 = 0.92$; see Supporting Information) and yielded a solvatochromic shift of 160 cm^{-1}, which is slightly lower than that of the Pt counterpart **3b**. The higher energy of the solvatochromic transition in **3a** relative to that of **3b** (543 nm) is consistent with significant metal orbital involvement in this transition.

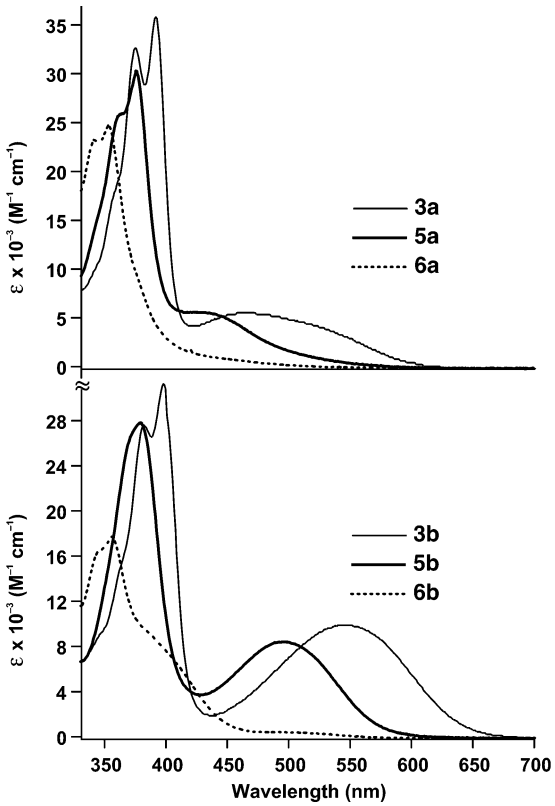

Figure 9. Electronic absorption spectra of complexes **3**, **5**, and **6a** (top) and **3**, **5**, and **6b** (bottom) in CH_2Cl_2 solution at 298 K.

Table 8. Lowest-Energy Absorption Band for Complexes **3a** and **b** and **5a** and **b** as a Function of Solvent[a]

	λ_{max} (nm)			
solvent	**3a**	**3b**	**5a**	**5b**
toluene	545	607	417	466
THF	497	564	419	470
$CHCl_3$	509	572	416	469
CH_2Cl_2	467	543	431	494
Me_2CO	451	528	417	470
dimethylsulfoxide	433	511	425	466
MeCN	446	502	425	463

[a] 5×10^{-5} M, except for **5b** in dimethylsulfoxide, which is 1.5×10^{-4} M.

The coordination of one $[Au(PCy_3)]^+$ unit to **3a** and **b** to give the dinuclear complexes **5a** and **b** causes significant modifications of the absorption spectra (Figure 9). The spectrum of **5a** in CH_2Cl_2 shows that the dithiolate-based bands broaden and blue shift to 359 and 376 nm, while for **5b** only one relatively broad band at 379 nm is observed. This blue shift points to an important involvement of the sulfur orbitals, most probably in the $\pi-\pi^*$ transitions. The broad lowest-energy absorption is centered at 431 nm for **5a** and 495 nm for **5b**. It is very similar in shape to the solvatochromic band of **3a** and **b** but significantly blue-shifted and has a somewhat lower molar extinction coefficient. Again, the energy of this transition is higher for the

(45) Karlin, K. D.; Stiefel, E. I. *Progress in Inorganic Chemistry. Dithiolene Chemistry: Synthesis, Properties, and Applications*; Wiley-Interscience: New York, 2004; Vol. 52.
(46) Cummings, S. D.; Cheng, L. T.; Eisenberg, R. *Chem. Mater.* **1997**, *9*, 440−450.
(47) Bereman, R. D.; Nalewajek, D. *Inorg. Chem.* **1976**, *15*, 2981−2984.

Pd complex **5a** than for its Pt analog **5b**, which supports metal orbital involvement and is consistent with a charge transfer to diimine, for which the mixed metal/dithiolate HOMO has a lower energy than that in **3a** and **b** because of the coordination of one of the sulfur atoms to a $[Au(PCy_3)]^+$ unit. The absorption spectra of **5a** and **b** in solvents of different polarity showed that the energy of this band undergoes only minor variations that do not follow a regular trend (Table 7); it is centered at around 420 (**5a**) or 470 nm (**5b**) in most solvents, and in both cases, the largest divergence is found in CH_2Cl_2 (431 or 495 nm, respectively). The drastically diminished solvatochromism of **5a** and **b** as compared to that of the parent complexes **3a** and **b** is attributable to a considerable loss of polarity as a consequence of the coordination to a $[Au(PCy_3)]^+$ unit. The changes in polarity between the ground and excited states are thus expected to be small and not to have a significant effect on the solvation of the cationic complexes **5a** and **b**.

The dithiolate-based absorptions undergo an additional shift to higher energies on going from **5a** and **b** to **6a** and **b** (Figure 9), appearing as two relatively broad and very close bands at 341 and 353 nm for **6a** or 343 and 356 nm for **6b** in CH_2Cl_2. These data confirm that the sulfur orbitals are involved in this transition and that their energy decreases as additional $[Au(PCy_3)]^+$ units are bonded to the dithiolato ligand. The shoulder at 397 nm observed for the Pt complex **6b** most probably corresponds to the charge transfer to diimine transition, which, as expected, is significantly blue-shifted relative to the monoaurated derivative **5b**. The corresponding absorption is not observed for the Pd complex **6a**, probably because it is obscured by the dithiolate-based bands.

The electronic absorption spectra showed that complexes **5a** and **b** and **6a** and **b** undergo dissociation of $[Au(PCy_3)]^+$ units in different solvents. For the monoaurated complexes **5a** and **b**, the dissociation of $[Au(PCy_3)]^+$ units is detectable in DMSO solution at concentrations below 2×10^{-4} M because it causes a red shift of the broad lowest-energy absorption band because of increasing concentration of the mononuclear precursors **3a** and **b**. The complete dissociation was observed at a concentration of 5×10^{-5} M in DMSO, DMF, and PrCN. In contrast, the absorption spectra of **5a** and **b** showed no significant shifts of the charge transfer to diimine absorption maximum in toluene, CH_2Cl_2, $CHCl_3$, THF, Me_2CO, and MeCN at different concentrations in the range of $10^{-4}-10^{-5}$ M, indicating that in these solvents the complexes are essentially stable.

The dissociation of $[Au(PCy_3)]^+$ units from the diaurated derivatives **6a** and **b** to give **5a** and **b** was observed in all the tested solvents. In the case of the Pt complex **6b**, the degree of dissociation α can be determined by using the absorbance values of the charge transfer to diimine absorption maximum arising from **5b**. However, for the Pd complex **6a** the absorbance of the corresponding band of **5a** could not be determined accurately, because this band is partially overlapped by the dithiolate-based absorptions and appears as a broad tail. At initial concentrations of around 5×10^{-5} M, the value of α for **6b** is very low in CH_2Cl_2 (0.06), while it is close to 0.40 in toluene, acetone, and THF and reaches 0.77 in MeCN. The observed tendency is consistent with the formation of solvent complexes of the type $[Au(PCy_3)(solvent)]^+$, which should be favored by the solvents with a better coordination ability toward Au(I). It must also be noted that higher values for α are obtained if the solvents are not rigorously dry. The effect of the concentration on the dissociation of **6b** was evaluated for THF solutions in the range from 2.2×10^{-5} to 3.1×10^{-4} M. As commonly observed for dissociation equilibria, the value of α was found to increase as the initial concentration of **6b** decreased (see Supporting Information for details). However, a consistent value for the dissociation constant could not be obtained, probably because of the instability of the cationic species $[Au(PCy_3)(solvent)]^+$.

Table 9. Excitation and Emission Data for **2a**, **2b**, **3b**, **4a**, **4b**, **5b**, and **6b**[a]

compd	medium (T/K)	λ_{exc} (nm)	λ_{em} (nm)	τ (μs)[c]
2a	solid (77)	*395*, 456, 485	690	198
	DMM (77)	434, 451, *466*	686	197
2b	solid (298)	363,456, *554*	618	10
	solid (77)	366, 456, *537*	632	73
	DMM (77)	456, *510*	*589*, 602	155
3b	solid (298)	415, 521, 557, *612*	730	< 10
	solid (77)	372, 391, 413, *466*, 601	*689*, 730[b]	9, 18[d]
	toluene (77)	380, *403*, 529, 580	673	6, 28[d]
	CH_2Cl_2 (77)	*380*, 400, 500, 533, 580	*673*, 732	9, 52[d]
4a	solid (77)	400, 432, *466*, 501	718	111
	DMM (77)	405, *431*, 455	722	88
4b	solid (298)	370−500	665	<10
	solid (77)	436, 461, 498	668	43
	DMM (77)	471	*609*, 670	127
5b	solid (298)	367−511	*605*, 664	51
	solid (77)	*366*, 518	*603*, 658	87
	toluene (77)	375, *396*, 477, 522	*609*, 663	38, 121[d]
	CH_2Cl_2 (77)	*369*, 396, 477, 513	*604*, 663	125
6b	solid (298)	375, 503	*608*, 658[b] (see text)	
	solid (77)	*367*, 428	*578*, 627	183
	toluene (77)	*351*, 398[b]	*566*, 618	270
	CH_2Cl_2 (77)	*354*, 399	*564*, 616	346

[a] The most intense peak is italicized. [b] Shoulder. [c] ±10%. [d] Double exponential.

Excitation and Emission Spectra. The compounds **2a**, **4a** and **b**, **5b**, and **6b** are photoluminescent at 77 K, and their excitation and emission spectra have been measured both in the solid state (polycrystalline samples) and in DMM (DMF/CH_2Cl_2/MeOH 1:1:1) glasses or frozen CH_2Cl_2 solutions. Room-temperature luminescence in the solid state was observed for the Pt/Au complexes **4b**, **5b**, and **6b**, whereas only the diimine complex **5b** displayed detectable luminescence in fluid CH_2Cl_2 solution at 298 K. The results of the measurements are summarized in Table 9. The Pd complexes **3a**, **5a**, and **6a** showed no emission at 77 K either in the solid state or in solution. The previously reported luminescence data of the Pt complexes **2b** and **3b**[18] are included in Table 9 for comparison.

The excitation and emission spectra of the Pd complexes **2a** and **4a** in DMM glass at 77 K are shown in Figure 10. In both cases, the lowest-energy excitation peaks approximately coincide in energy with the corresponding MLCT absorptions. The emission spectra show a symmetrical band with a full width at half-height of 1474 (**2a**) or 1267 cm^{-1} (**4a**)

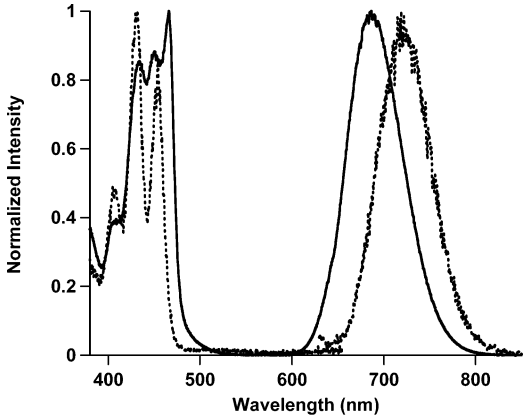

Figure 10. Excitation and emission spectra of complexes **2a** (—) and **4a** (· · ·) in DMM glasses at 77 K.

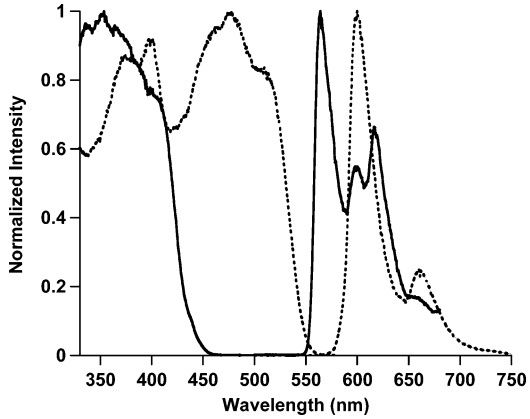

Figure 11. Excitation (left) and emission (right) spectra of a frozen solution of **6b** in CH_2Cl_2 at 77 K. The emission spectra were registered with excitations at 352 (—) or 477 nm (· · ·). The spectra represented as dotted lines coincide with the excitation and emission spectra of **5b**.

and no discernible vibronic structure. The band maximum is at 686 (**2a**) or 722 nm (**4a**), which leads to very large Stokes shifts of 6882 or 8128 cm^{-1}, respectively. Polycrystalline samples of **2a** and **4a** at 77 K displayed emission spectra that are very similar to those obtained in DMM glasses. The large Stokes shifts, lack of vibronic structure and long decay lifetimes in the microsecond range are consistent with an essentially metal-centered ^{3}d−d emitting state.[48] As far as we are aware, there are no previous reports on the luminescence of Pd(II) complexes with 1,1-ethylenedithiolato ligands. The dianionic 1,2-dithiolene complex $[Pd(mnt)_2]^{2-}$ displays luminescence at 77 K, which arises from a triplet excited-state involving a LUMO of essentially d orbital character and a HOMO of mixed Pd(d)/$\pi_{dithiolate}$ orbital character.[49] Analogous frontier orbital designation and luminescence assignment seem appropriate for **2a** in view of the particular electronic properties of (fluoren-9-ylidene)-methanedithiolato ligands, which have proved to be similar to those of 1,2-dithiolenes in electron-donating ability.[18] Thus, although the lowest-energy absorption observable for **2a** arises from a charge-transfer transition between the mixed metal/dithiolate HOMO and a dithiolate-based π^* orbital, the LUMO is essentially the vacant d orbital of Pd, and a state that can be approximately designated as ^{3}[Pd(d)/$\pi_{dithiolate}$−Pd(d)] becomes the emitting state. The coordination of two $[Au(PCy_3)]^+$ units and the formation of relatively strong metallophilic contacts in **4a** have the effect of decreasing the emission energy. We have also considered the possibility that the emission of **2a** arises from an intraligand transition. However, the characteristics of this emission and the fact that its energy decreases upon coordination of two $[Au(PCy_3)]^+$ units do not favor such an assignment. Alkaline salts of the (2,7-di-*tert*-butylfluoren-9-ylidene)methanedithiolate ligand could not be isolated, and therefore their emission spectra are not available. The compound [2,7-bis(octyloxy)fluoren-9-ylidene]methanedithiol displays an emission maximum at 525 nm at 77 K both in the solid state and in frozen CH_2Cl_2, most probably associated with the C═CS_2 moiety.[16,24] An emission of similar shape and energy is observed for $(Bu_4N)_2[Zn\{S_2C{=}(t\text{-Bu-fy})\}_2]$ (522 nm) and probably has the same origin.[50] A triplet emission from the fluoren-9-ylidene group should be expected at a higher energy.[51]

The emission spectrum of the Pt/Au complex **4b** in DMM glass at 77 K is drastically different from that of its Pd/Au counterpart **4a**, showing one sharp absolute maximum at 609 nm and a less intense peak at 670 nm. The corresponding excitation spectrum shows the absolute maximum at 471 nm, which coincides in energy with the lowest absorption band in CH_2Cl_2. The vibronic spacing of 1495 cm^{-1} is comparable to that observed for the mononuclear precursor **2b**[18] and suggests a similar origin for the emission of **4b**, that is, a ^{3}MLCT excited state, most probably perturbed by the metallophilic interactions. The decay lifetimes of **2b** and **4b** (Table 9) are also similar to each other and consistent with excited states of triplet parentage.

The measurement of the excitation and emission data for the Pt/Au complexes **5b** and **6b** in solution was problematic because of their tendency to lose $[Au(PCy_3)]^+$ units in glass-forming solvents such as PrCN and 2-methyltetrahydrofuran or solvent mixtures such as EtOH/MeOH and DMM. To minimize dissociation, the solution measurements at 77 K were made in frozen CH_2Cl_2 and toluene glasses. Complex **5b** displays a bright orange luminescence in the solid state at 298 and 77 K, which can even be observed under normal room illumination. Its emission spectrum shows very similar profiles in the solid state and in frozen CH_2Cl_2 at 77 K, with an absolute maximum at 605 nm and a less intense peak at 660 nm (Figure 11). The emission in fluid CH_2Cl_2 solution at 298 K is very weak and has a much broader shape, but the energies of the two maxima coincide with those observed at 77 K. The excitation spectra of **5b** in both frozen and fluid CH_2Cl_2 closely reproduce the absorption spectrum in CH_2Cl_2 at 298 K but are broad and complicated in the solid state. Since the formation of π-stacked dimers of **5b** at the low concentrations employed for the solution measurements ($\sim 5 \times 10^{-5}$ M) is expected to be negligible at 298 K, the

(48) Crosby, G. A. *Acc. Chem. Res.* **1975**, *8*, 231−238.
(49) Güntner, W.; Gliemann, G.; Kunkely, H.; Reber, C.; Zink, J. I. *Inorg. Chem.* **1990**, *29*, 5238−5241.
(50) González-Herrero, P.; García-Sánchez, Y. Unpublished results.
(51) Vo-Dinh, T.; Gammage, R. B. *Anal. Chem.* **1978**, *50*, 2054−2058.

present data indicate that π-stacking does not have a substantial effect on the emission energy of this complex. The observed emission of polycrystalline **6b** at 298 K is almost identical (although broader) to that of **5b**. However, at 77 K, two distinct emissions can be observed both in the solid state and in frozen CH_2Cl_2. When excited at a 475 nm or longer wavelength, the emission profile coincides with that of **5b**; but at an excitation wavelength of 400 nm or shorter, the most intense emission bands occur at 564 and 616 nm (CH_2Cl_2) or 578 and 627 nm (solid) and overlap two less intense peaks ar 600 and 660 nm (Figure 11). It is reasonable that the higher-energy emission corresponds to the diaurated complex **6b**, which is supported by the fact that the excitation spectrum collected at the 564 nm emission maximum in frozen CH_2Cl_2 approximately coincides with the absortion spectrum of **6b** in fluid solution. The lower-energy emission would then arise from small amounts of **5b**, which result from the dissotiation of $[Au(PCy_3)]^+$ units in CH_2Cl_2 solution. In fact, the emission spectrum of **6b** in toluene glass at 77 K registered at an excitation wavelength of 352 nm also shows the two emissions, but the relative intensity of the bands arising from **5b** is higher because of the greater dissociation degree in this solvent compared to that in CH_2Cl_2. The presence of **5b** in polycrystalline samples of **6b** may be associated with partial decomposition in the solid state, and it is likely that the observed luminescence at 298 K is dominated by the much more intense emission of **5b**. The decay lifetimes measured at 77 K are in the microsecond range and increase in the sequence **3b** < **5b** < **6b**.

The similarity of the emissions of **5b** and **6b**, with a single vibronic spacing, suggests an emitting state of common origin. This vibronic spacing varies between 1352 and 1497 cm^{-1}, depending on the medium, and thus lies within the range of 1200−1500 cm^{-1} typically observed for emissions that involve a diimine based π^* orbital in the excited state.[23,52,53] The increase in the emission energy in the order **3b** < **5b** < **6b** (CH_2Cl_2, 77 K) is attributable to a stabilization of the mixed metal/dithiolate HOMO as a consequence of the coordination of successive $[Au(PCy_3)]^+$ units. Therefore, the present data suggest that the luminescence of **5b** and **6b** involves a transition of the same orbital parentage as the charge transfer to diimine absorption, but from a triplet excited state. A similar assignment has been made for heteronuclear complexes of the type $[Pt(tdt)(diimine)\{M_2(dppm)_2\}]^{2+}$ [M = Ag, Au; tdt = 3,4-toluenedithiolate; dppm = 1,1-bis(diphenylphosphino)methane].[4] Nevertheless, the emissions of **5b** and **6b** most probably originate from a mixture of charge transfer to diimine and diimine intraligand $^3\pi-\pi^*$ contributions. The emissions of mononuclear Pt diimine complexes containing 1,1-ethylenedithiolates have been most frequently assigned to charge transfer to diimine triplet states,[23] although in some cases a mixed origin has been established, which includes both charge transfer to diimine and diimine-based $\pi-\pi^*$ triplet states.[21,54] An important contribution of the diimine-based $^3\pi-\pi^*$ state in **5b** and **6b** is reasonable because the coordination of **3b** to $[Au(PCy_3)]^+$ units increases the energy of the charge transfer to diimine transition, while the diimine $\pi-\pi^*$ gap is not expected to undergo significant variations upon modifications of the ligands attached to Pt,[23,53−55] and thus the two states should lie closer in energy than in the mononuclear precursor. The increasing contribution of the diimine $^3\pi-\pi^*$ state upon the coordination of successive $[Au(PCy_3)]^+$ units could account for the narrower and more defined vibronic structure of the emissions of **5b** and **6b**, compared to those of their mononuclear precursor **3b**, and probably also for their longer lifetimes. In fact, the emissions that originate from $^3\pi-\pi^*$ states are known to have typically very long lifetimes.[21,54]

Conclusions

The complexes $[M\{S_2C{=}(t\text{-Bu-fy})\}_2]^{2-}$ [M = Pd (**2a**), Pt (**2b**)] and $[M\{S_2C{=}(t\text{-Bu-fy})\}(dbbpy)]$ [M = Pd (**3a**), Pt (**3b**)] can act as metalloligands toward $[Au(PCy_3)]^+$ units to form heteronuclear complexes of the types $[M\{S_2C{=}(t\text{-Bu-fy})\}_2\{Au(PCy_3)\}_2]$ [M = Pd (**4a**), Pt (**4b**)], $[M\{S_2C{=}(t\text{-Bu-fy})\}(dbbpy)\{Au(PCy_3)\}]ClO_4$ [M = Pd (**5a**), Pt (**5b**)], and $[M\{S_2C{=}(t\text{-Bu-fy})\}(dbbpy)\{Au(PCy_3)\}_2](ClO_4)_2$ [M = Pd (**6a**), Pt (**6b**)]. The crystal structures of **4a**, **4b**, **5b**, and **6a** reveal that the $[Au(PCy_3)]^+$ units are bonded to one of the sulfur atoms of the dithiolato ligand and adopt similar arrangements, which lead to the formation of short Pd···Au or Pt···Au metallophilic contacts. The heteronuclear derivatives undergo a dynamic process in solution that involves the migration of the $[Au(PCy_3)]^+$ units between the sulfur atoms of the dithiolato ligands. The enthalpies of activation of these processes are higher for the Pd/Au systems than for their Pt/Au analogs, possibly because Pd···Au contacts have lower interaction energies and are thus less effective in assisting the migration than Pt···Au contacts. The coordination of **2a** and **b** and **3a** and **b** to $[Au(PCy_3)]^+$ units results in important modifications of their photophysical properties. The dominant effect that is observable in the absorption spectra is an increase in the energy of the MLCT (**4a** and **b**) or charge transfer to diimine (**5a** and **b**, **6a** and **b**) transitions because of a decrease in the energies of the mixed metal/dithiolate HOMOs. The characteristics of the emissions of the Pd complexes **2a** and **4a** are compatible with essentially metal-centered ^{3}d−d states. The emissions of the heteronuclear Pt/Au complexes can be assigned as originating from a MLCT triplet state (**4b**) or a mixture of charge transfer to diimine and diimine intraligand $\pi-\pi^*$ triplet states (**5b** and **6b**).

Acknowledgment. We thank Ministerio de Educación y Ciencia (Spain), FEDER (CTQ2004-05396) for financial

(52) (a) Caspar, J. V.; Kober, E. M.; Sullivan, B. P.; Meyer, T. J. *J. Am. Chem. Soc.* **1982**, *104*, 630−632. (b) Miskowski, V. M.; Houlding, V. H. *Inorg. Chem.* **1991**, *30*, 4446−52. (c) Miskowski, V. M.; Houlding, V. H.; Che, C. M.; Wang, Y. *Inorg. Chem.* **1993**, *32*, 2518−2524.

(53) Houlding, V. H.; Miskowski, V. M. *Coord. Chem. Rev.* **1991**, *111*, 145−52.

(54) Zuleta, J. A.; Bevilacqua, J. M.; Proserpio, D. M.; Harvey, P. D.; Eisenberg, R. *J. Am. Chem. Soc.* **1992**, *31*, 2396−2404.

(55) Connick, W. B.; Miskowski, V. M.; Houlding, V. H.; Gray, H. B. *Inorg. Chem.* **2000**, *39*, 2585−2592.

support. P.G.-H. thanks Ministerio de Educación y Ciencia (Spain) and Universidad de Murcia for a contract under the *Ramón y Cajal* Program. M.P.-C. thanks Ministerio de Educación y Ciencia (Spain) for a research grant.

Supporting Information Available: Crystallographic data in CIF format for **3a**·CH_2Cl_2, **4a**, **4b**, **5b**·Me_2CO, and **6a**·THF·C_6H_{14}, ^{1}H NMR spectra of complex **5a** at different concentrations, variable-temperature ^{1}H NMR spectra of **5a** and **b**, results of the line-shape analyses, including Eyring and Arrhenius plots, plot of the lowest absorption energy of **3a** versus the Pt(NN)(SS) solvent parameter, and plot of the degree of dissociation α versus concentration for **6b** in THF. This material is available free of charge via the Internet at http://pubs.acs.org.

IC070164H